Check for updates

RESEARCH ARTICLE

High Resolution Global Environmental Stratification to Model Shifting Bioclimatic Conditions and Climate Change Impacts on Terrestrial Ecosystems

[version 1; peer review: 1 approved]

Robert J. Zomer[1,2], Marc J. Metzger[3], Jianchu Xu[2,4], Antonio Trabucco[1,5]

[1]CMCC Foundation – Euro-Mediterranean Center on Climate Change, Sassari, Italy
[2]Center for Mountain Futures, Kunming Institute of Botany, Kunming, Yunnan, China
[3]School of GeoSciences, The University of Edinburgh, Edinburgh, Scotland, UK
[4]China Program, CIFOR-ICRAF, Kunming, Yunnan, China
[5]National Biodiversity Future Center (NBFC), Palermo, Sicily, Italy

v1 **First published:** 25 Jul 2025, **5**:193
https://doi.org/10.12688/openreseurope.20387.1
Latest published: 25 Jul 2025, **5**:193
https://doi.org/10.12688/openreseurope.20387.1

Abstract

Background

Understanding climate-driven ecological change benefits from frameworks capable of translating climate model outputs into ecologically interpretable spatial patterns. This study presents a global application of the Environmental Stratification (EnS) methodology, using Maximum Likelihood Classification, and integrating outputs from 22 CMIP6 Earth System Models (ESMs) across four Shared Socioeconomic Pathways (SSP: 1-2.6; 2-4.5; 3-7.0; 5-8.5), two historical baseline climate datasets (1960–1990; 1970–2000), and two future averaged time periods (2021–2040; 2041–2060). Both "Consensus" and "High-Risk" multimodel majority ensembles were selected and used in the global analysis. The resulting *Future_Global_EnS Database* (https://doi.org/10.5281/zenodo.15099763), provides these highresolution EnS projections at 30 arc seconds resolution (~1km^2). The global EnS analysis reveals extensive bioclimatic reorganization by mid-century. Cooler and mesic zones, particularly boreal, temperate, and montane systems, exhibit high zonal turnover, significant poleward latitudinal shifts, upslope migrations, and mountaintop extirpations. Tropical, arid, and extremely hot zones show significant spatial expansion and internal reorganization under high-emissions scenarios, including large-scale growth of drylands and intensification of extremely hot bioclimatic conditions. Results from the global EnS

Open Peer Review

Approval Status ✓

	1
version 1 25 Jul 2025	✓ view

1. **Vivek Chetry**, Gauhati University, Guwahati, India

Any reports and responses or comments on the article can be found at the end of the article.

analyses align closely with empirical observations of bioclimatic and ecological shifts, providing spatially explicit, ecologically grounded metrics for anticipating where and how terrestrial ecosystems will change. By delineating statistically based coherent and ecologically meaningful geospatial strata, the EnS methodology provides a powerful tool for translating complex climate projections into interpretable ecological insights and enables rigorous analysis of climate impacts at decision-relevant scales. Both the EnS methodology and *Future_Global_EnS Database* provide a resource with immediate utility for biodiversity conservation, land-use policy, agricultural sustainability, natural resource management, and adaptation to rapid climate change, at global to regional and local scales.

Plain Language Summary

As the planet warms, natural systems across the globe are shifting, and this study introduces a widely applicable methodology and a new global dataset that helps us understand how climate change is expected to alter the environments where plants and animals live. Using climate projections, the researchers mapped how bioclimatic zones—areas with similar temperature, rainfall, and moisture—are likely to shift over time. This method, called Environmental Stratification (EnS), identifies patterns such as cold, wet forests or hot, dry deserts, and shows how these zones may move, shrink, or expand in the coming decades. For instance, cooler zones in mountains and polar regions are projected to decline, while hotter and drier zones are expected to grow. Many regions may experience climates that differ significantly from the past, with shifts occurring toward the poles or higher elevations. These changes affect agriculture, biodiversity, and water resources, especially in areas already vulnerable to climate extremes. The analysis highlights patterns of bioclimatic displacement, zone turnover, and emerging risk space, offering a global-scale perspective on the pace and direction of ecological change under climate warming.

While the main contribution is the utility of the EnS framework in interpreting future climate conditions, the study also makes available a high-resolution (30 arc-second) global dataset of present and projected EnS classifications. This open-access resource supports research, planning, and decision-making related to conservation, land management, and climate adaptation.The new EnS database stands out for its global coverage, high spatial detail (about 1 km resolution), and public accessibility, making it a useful tool for governments, researchers, land managers, and communities preparing for future conditions. The work reflects a collaboration between European and Chinese institutions, particularly the Center for Mountain Futures at the Kunming Institute of Botany and the CMCC Foundation in Italy, and provides a practical resource for supporting climate adaptation.

Keywords
Bioclimatic zones, climate change impacts, ecological modeling, adaptation

H2020 This article is included in the Horizon 2020 gateway.

Corresponding author: Robert J. Zomer (robert.zomer@cmcc.it)

Author roles: Zomer RJ: Conceptualization, Data Curation, Formal Analysis, Methodology, Software, Validation, Visualization, Writing – Original Draft Preparation, Writing – Review & Editing; **Metzger MJ**: Conceptualization, Methodology, Writing – Review & Editing; **Xu J**: Funding Acquisition, Writing – Review & Editing; **Trabucco A**: Conceptualization, Formal Analysis, Funding Acquisition, Methodology, Software, Validation, Writing – Original Draft Preparation, Writing – Review & Editing

Competing interests: No competing interests were disclosed.

Grant information: This project has received funding from the European Union's Horizon 2020 Research and Innovation Programme under grant agreement No ([Grant No. 101036683] [TRANSFORMAR]; [Grant No. 101003881] [NEXOGENESIS]) and the National Recovery and Resilience Plan of Italian Ministry of University and Research funded by NextGenerationEU (NBFC Grant No. CN_00000033). Additional support by National Science Foundation China-CGIAR Project (Grant No. 31861143002) and the Yunnan Provincial Science and Technology Department (Grant No. 202303AP140001).
The funders had no role in study design, data collection and analysis, decision to publish, or preparation of the manuscript.

Copyright: © 2025 Zomer RJ *et al*. This is an open access article distributed under the terms of the Creative Commons Attribution License , which permits unrestricted use, distribution, and reproduction in any medium, provided the original work is properly cited.

How to cite this article: Zomer RJ, Metzger MJ, Xu J and Trabucco A. **High Resolution Global Environmental Stratification to Model Shifting Bioclimatic Conditions and Climate Change Impacts on Terrestrial Ecosystems [version 1; peer review: 1 approved]** Open Research Europe 2025, **5**:193 https://doi.org/10.12688/openreseurope.20387.1

First published: 25 Jul 2025, **5**:193 https://doi.org/10.12688/openreseurope.20387.1

Introduction

Given ongoing and accelerating global climatic change[1], and our current climate emergency[2–4], the need for robust methodologies to assess impacts on terrestrial ecosystems[5] and associated biological[6] and human systems[7], is ever more relevant and increasingly more urgent. Environmental stratification, or more specifically, the "EnS" environmental stratification methodology[8–11] provides a structured approach to modeling interactions between climate variables and terrestrial landscapes. This method is, among other equally relevant applications, well suited to analyzing potential changes in vegetated landscapes[12], where shifts in temperature, precipitation, and other bioclimatic factors can influence ecosystem structure[13] and function[14,15]. The integration of environmental stratification with predictive modeling, combined with parameterization and validation from a variety of thematically or geographically specific empirical or modeled datasets[16], can provide an improved understanding of how climate change and shifting bioclimatic conditions may alter ecological patterns and processes for both natural[13,17] and managed systems[9]. Understanding these changes in ecological processes is fundamental to developing effective human adaptation strategies to climate change[18].

Ecosystems respond dynamically to shifting bioclimatic conditions[5], influencing biodiversity, ecosystem services, and resource availability, which in turn affect human societies[6]. By integrating predictive modeling with ecological monitoring, policymakers and stakeholders can anticipate bioclimatic shifts and their impact on ecosystem structure and function[19], allowing for proactive adaptation measures in biodiversity conservation[20,21], agriculture[22,23], water resource management[24], rural development and urban planning[18,19]. For example, ecosystem-based adaptation strategies (EbA) and other Nature Based Solutions (NbS)[25], such as restoring wetlands to mitigate floods or implementing agroforestry systems to enhance soil conservation[26], have been shown to enhance both ecological and human resilience to climate stressors. However, integrating these approaches into appropriate policies requires a comprehensive approach and context-aware understanding[27]. Additionally, studies indicate that transformative adaptation, where fundamental changes in land use and resource management are implemented, can be necessary in regions experiencing extreme ecological shifts[28]. A predictive understanding of how climate change modifies future bioclimatic conditions[29], and consequently interactions in social-ecological and other human systems[18], leading to shifts in system trajectories, can help identify appropriate adaptation responses, including transformative adaptation, that provide long-term and sustainable benefits. Predictive and integrative modeling incorporating environmental and bioclimatic stratification[12,30,31] can provide valuable insights and inputs for facilitating interdisciplinary approaches that combine ecological science, climate modeling, and socio-economic planning to develop robust adaptation frameworks[18,19,32] through delineating future risk space[33–35] in highly interpretable bioclimatic and ecological terms.

Environmental stratification

Environmental stratification involves the partitioning of the Earth's surface into relatively homogeneous zones based on a range of bioclimatic and environmental variables[36,37]. These zones, or strata, are characterized by distinct bioclimatic and/or other biophysical (or socio-economic/socio-ecological) conditions[38] that influence the distribution and dynamics of terrestrial ecosystems. Environmental stratification has evolved from traditional biogeographical classification systems, tracing its roots to the 19th and early 20th centuries. Researchers such as Alexander von Humboldt[39] and Wladimir Köppen[40] developed climatic classification frameworks that laid the groundwork for understanding spatial environmental variability. Köppen's climate classification system[40], introduced in 1900, became one of the earliest systematic approaches to delineating ecological regions based on temperature and precipitation patterns. By the mid-20th century, advances in ecological modeling and statistical analysis facilitated more refined stratification approaches[41], integrating topographic, soil, and land-use factors[42]. The advent of geographic information systems (GIS) and the increasing availability of climatic and other earth observation data in the latter half of the 20th century allowed for the delineation of environmental strata with increasing precision[43]. Environmental stratification is now widely applied in various scientific and other fields, providing a structured framework for analyzing complex interactions between biotic and abiotic components of the environment. More recently, environmental stratification methodologies have been integrated with machine learning and remote sensing technologies, enabling more dynamic and predictive modeling of ecological processes. A prime utility of global environmental stratification is its ability to synthesize climatic data into coherent and interpretable spatial models that can be applied across diverse geographic regions[36,44,45].

The "Global Environmental Stratification" (GEnS)

Metzger *et al.*[10] produced the "Global Environmental Stratification" (GEnS) dataset[46] with the aim to provide a robust and global spatial analytical framework for the aggregation of local observations, identification of gaps in current monitoring efforts and systematic design of complementary and new monitoring and research. The GEnS was originally developed to support global biodiversity monitoring and ecosystem research within the framework of the Group on Earth Observations Biodiversity Observation Network (GEO-BON) and has since been the basis for numerous studies on a variety of topics[9,12,17,20,21,47–49]. The GEnS classifies the world's land surface into 125 relatively homogeneous bioclimatic strata, which cluster areas with similar bioclimates together, using a statistical analysis of historical climate data based on the WorldClim[50] climate datasets. The WorldClim dataset is based on weather station monthly climate data geospatially interpolated to 30 arc seconds (~ 1 km^2) resolution using latitude, longitude and elevation as independent variables, and averaged over a 30-year time period.

To produce the original GEnS, Metzger *et al.*[10] identified a subset of 36 biophysically relevant bioclimatic variables based on a statistical screening of 42 variables available from various climate geodatasets. Principal Components Analysis revealed that the first three principal components[10,51,52], explaining 99.9% of the total variation, were determined by only four variables.

- Tmean Degree Days > 0°C[50,53]
    - daily sum of annual degrees of temperature above 0°C, reflecting latitudinal and altitudinal temperature gradients, and plant growth periods;
- Aridity Index (AI)[54,55]
    - ratio of annual precipitation over annual potential evapotranspiration (PET; calculated globally using the Hargreaves model)
- Monthly Mean Temperature Seasonality[50,53]
    - standard deviation of the monthly mean temperature distribution
- PET Seasonality[54,55]
    - standard deviation of the monthly mean PET distribution

A full description of the GEnS methodology, along with a detailed discussion of its conservation and environmental monitoring utility is given in Metzger *et al.*[10,44], with further elaboration within the context of identifying agroclimatic zones and meeting regulatory requirements provided by Melnick *et al.*[56]. In the modeling and analysis presented in this paper, the GEnS dataset and its taxonomy is replicated and utilized as a starting point.

Environmental stratification and predictive modeling

Environmental stratification as a methodology not only enhances our understanding of current ecosystem patterns but also can provide a basis for forecasting future changes in response to ongoing and projected climatic shifts and/or other environmental changes. One of the key strengths of a statistical non-subjective environmental stratification is its capacity to integrate multiple climatic, bioclimatic, and other environmental variables into a unified, statistically derived framework, allowing ecologically interpretable results, as well as comparative studies and identification of bioclimatically similar or homologous strata. The resulting strata, or global zonation, while being of high utility describing current and historical conditions, also provide a baseline and, importantly, a starting point for predictive modeling efforts. Since the GEnS uses a purely quantitative statistical approach to characterize bioclimatic strata, the statistical classification methodology can be applied in a similar manner to develop a similar stratification based upon predicted future climate conditions.

By applying the same clustering algorithm and strata-specific signature profiles derived from the original GEnS strata (i.e. based upon the historical climate data) to future climate projections, the environmental stratification models can simulate potential future scenarios, providing insights into how different climate trajectories might influence the distribution of bioclimatic zones, vegetation[12], hydrological cycles, and the overall functioning of ecosystems, among others impacts. While maintaining appropriate caution regarding the variability associated with future climate models and projections, such predictions can be of great utility for adaptation or biodiversity conservation planning, as they allow for the identification of areas that are most vulnerable to climate-induced changes and the development of strategies to mitigate these impacts. The stratification approach can provide insight into non-linear and synergistic effects of climate change on ecosystems. For example, changes in precipitation patterns may interact with rising temperatures to exacerbate drought conditions, leading to widespread vegetation die-off in certain regions. Conversely, in other areas, increased moisture availability could enhance plant growth, potentially altering competitive dynamics among species and leading to shifts in community composition. By summarizing these conditions geographically and allowing interpretation of changing bioclimatic conditions based upon a comparison of existing similar conditions elsewhere, environmental stratification provides the opportunity to project and understand how climate change, based upon the existing climate projections, will reshape the Earth's landscapes bioclimatically, and by extension, ecologically. In this paper, we apply the EnS methodology to identify bioclimatic shifts, using the GEnS framework as a starting point, comparing an overview of global results for two historical datasets (1960–1990; 1970–2000), future projected climate data from 22 CMIP Phase 6 Earth System Models (ESMs), and two multi-model ensembles (Consensus, High Risk) with uncertainty measures linked to climate model agreement (Figure 1), across four Shared Socioeconomic Pathways (SSP: 1-2.6, 2-4.5, 3-7.0, 5-8.5).

Methods

EnS bioclimatic stratification

A statistically derived bioclimatic stratification, which we refer to here as "EnS" to differentiate our results from the original GEnS, but based on the GEnS dataset produced by Metzger *et al.*[10], was used to predict and understand the nature and magnitude of projected changes in the spatial distribution of bioclimatic conditions globally. The modeling approach[9,48] reconstructs a high resolution global EnS bioclimatic stratification based on the statistical profiles of the original GEnS strata and zones. Both the geospatial classification of the GEnS dataset and its associated taxonomy of bioclimatic strata were used as the starting point, training dataset, and overall context for the reconstructed EnS bioclimatic stratification based on historical and projected future climatic conditions.

The EnS analysis uses the same four variables as used to derive the original GEnS, as described above, to reconstruct the global EnS, using both historical and projected future climatic datasets. To develop the reconstructed (global) EnS stratification first for the historical period of 1960–1990 and then for the 1970–2000 time period, which is used as the comparative baseline in this analysis, the four selected variables were used to develop profiles and reconstruct the EnS strata based on the original GEnS and the WorldClim v1.4 dataset (for 1960–1990) as originally used in the GEnS analysis. An iterative statistical clustering method learning technique (ISODATA)[57,58] was used to stratify (cluster) the globe into 125 strata, aggregated into 18 zones, to construct this baseline EnS dataset for 1970–2000. Consistent descriptive names were attributed to strata and zones based upon the original GEnS taxonomy, with first letters (in alphabetical order)

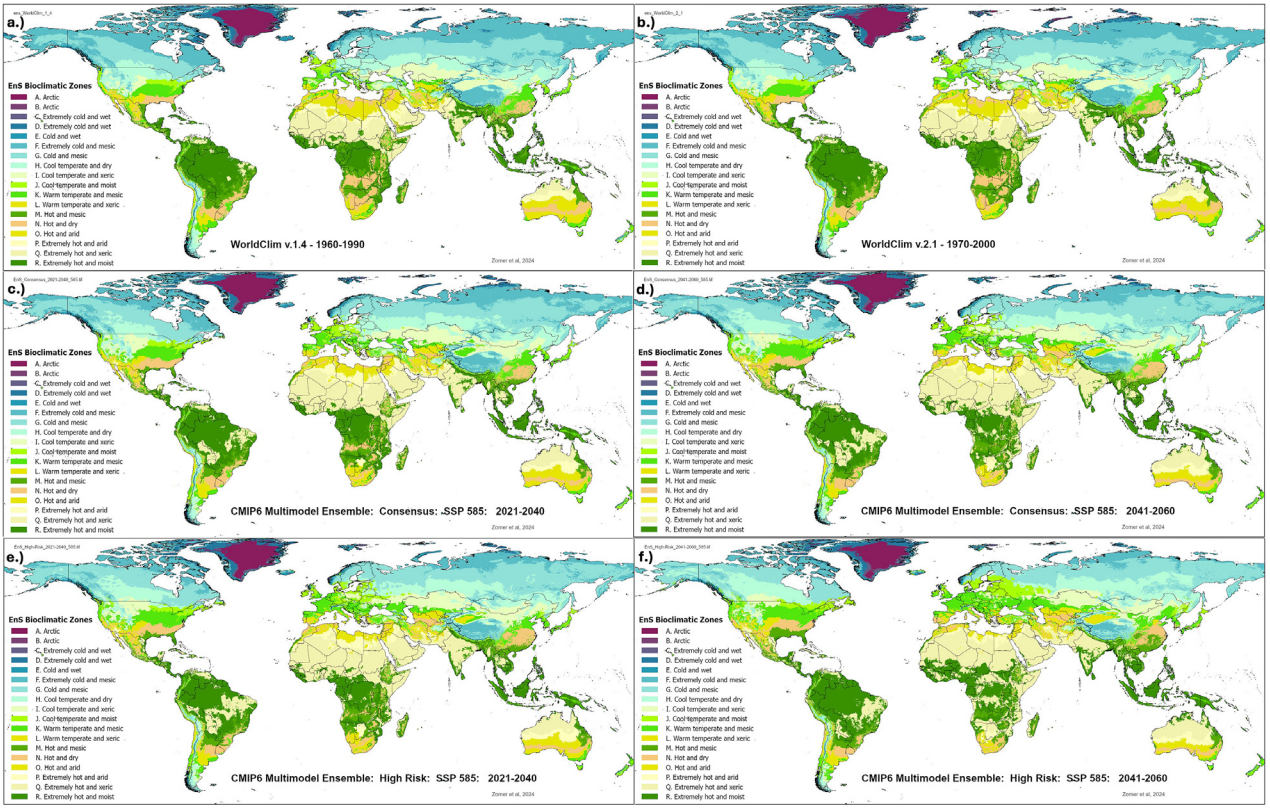


Figure 1. Future_Global_EnS_Database – historical and projected environmental stratification (EnS) datasets developed and used in the global analysis. EnS bioclimatic stratification for two historical periods: **a.**) 1960–1990; **b.**) 1970–2000. EnS bioclimatic stratification for CMIP Phase 6 Earth System Models projections, here illustrated with examples for two future time periods for the "Consensus" and the "High Risk" Ensembles: **c.**) Consensus Ensemble for 2021–2040; **d.**) Consensus Ensemble for 2041–2060; **e.**) High Risk Ensemble for 2021–2040; **f.**) High Risk Ensemble for 2041–2060.

and lower numbers characterizing colder zones and strata. Statistical signature profiles were derived from the original GEnS dataset (which was based upon WorldClim 1.4) using the Maximum Likelihood Classification algorithm in ArcGIS 10.8 (ESRI).

Based on the confusion matrix comparing the original GEnS data versus the reconstructed EnS classification (for 1960–1990, i.e. WorldClim v 1.4), the overall user accuracy for the EnS bioclimatic strata was 91.7% and the Kappa Coefficient (k-Cohen) was 0.916. This compared favorably to other similar efforts[59]. Soteriades *et al.*[11] compared several alternative classifiers on a similar dataset, identifying Random Forest Classifier[60] as the most accurate and appropriate for their approach. However, in this case, none of the methods tested matched or exceeded the results obtained using the Maximum Likelihood Classifier using the four variables identified in the construction of the original GEnS. This was perhaps influenced by the coarser resolution of their datasets.

The signature profiles of the original GEnS strata obtained from the Maximum Likelihood Classifier were used to reconstruct the EnS stratification based first on the WorldClim v1.4 dataset, to evaluate the accuracy of the classification. Then, these were used to classify the WorldClim v2.1 dataset, to develop the EnS WC_2.1 historical baseline dataset, representing the averaged time period of 1970–2000, and then for all of the selected 22 CMIP6 ESM for each of the two time periods included in this study (2021–2040; 2041–2060). Zomer *et al.*[9,17] outlines a detailed presentation of the EnS stratification methodology and its application to future climate projection data, as used in this study, and described below.

Modeling of projected future climate conditions

Projected impacts on bioclimatic conditions are modeled by reconstructing the global stratification based upon future climate conditions both as modeled by each individual CMIP6 ESM (n = 22) included in the study, and by two majority ensembles of ESM results[61]. Mora *et al.*[62] tested the robustness of averaged ensembles based on historical observation data (1985–2005) and found a higher correlation when using multi-model averages, echoing advice provided in IPCC AR5[63]. CMIP6 represents a significant advancement in climate modeling, incorporating more sophisticated representations of ice, water, and cloud dynamics compared to its predecessor, CMIP5. These models integrate a broader array of physical processes,

reflecting ongoing efforts to enhance the realism of climate projections. However, the IPCC has acknowledged an issue of "hot" models, wherein some projections suggest considerably higher levels of equilibrium climate sensitivity (ECS), that is, higher levels of future warming. Including these into averaged ensembles creates a risk of studies reporting projections that are overly influenced by the "hot models" and inconsistent with IPCC assessed warming averages[64]. The IPCC's Sixth Assessment Report (AR6)[1,65] considered this and reconciled the climate models used with observational data, including global mean temperature rise, sea-level changes, and ocean heat content. Using statistical methods, the IPCC derived projections that harmonize with multiple lines of empirical evidence, producing "assessed warming" estimates. For our analysis, 22 ESM were evaluated and identified (Table 1), considering the availability of downscaled CMIP6 ESM[50] and their transient climate response (TCR) rankings[66,67] Based upon the distribution of average global mean annual temperature and

Table 1. Available EnS Datasets in the *Future_Global_EnS_Database* Used in the Global EnS Analysis. Available datasets in the *Future_Global_EnS_Database*, developed and used in the global EnS analysis, including two historical datasets, 22 CMIP Phase 6 Earth System Models (ESM), calculated for each of their respective four Shared Socio-Economic Pathways (SSP: 1-2.6; 2-4.5; 3-7.0; 5-8.5), for two time periods (2021-2040; 2041-2060), and two multi-model majority ensembles (Consensus, High-Risk).

Historical Datasets									**ESMs included within Ensemble**		
WorldClim 1.4 (1960–1990)											
WorldClim 2.1 (1970–2000)											
Earth System Models (ESM)	**Year: 2021–2040**				**Year: 2041–2060**				**MultiModel Ensemble**		
SSP Scenario:	**126**	**245**	**370**	**585**	**126**	**245**	**370**	**585**	**All**	**Consensus**	**High-Risk**
ACCESS-CM2	X	X	X	X	X	X	X	X	X		X
ACCESS-ESM1-5	X	X	X	X	X	X	X	X	X	X	
CanESM5	X	X	X	X	X	X	X	X	X		X
CanESM5-CanOE	X	X	X	X	X	X	X	X	X		X
CMCC-ESM2	X	X	X	X	X	X	X	X	X	X	
CNRM-CM6-1	X	X	X	X	X	X	X	X	X	X	
CNRM-CM6-1-HR	X	X	X	X	X	X	X	X	X	X	
CNRM-ESM2-1	X	X	X	X	X	X	X	X	X	X	
FIO-ESM-2-0	X	X		X	X	X		X	X		
GFDL-ESM4	X		X		X		X		X		
GISS-E2-1-G	X	X	X	X	X	X	X	X	X	X	
GISS-E2-1-H	X	X	X	X	X	X	X	X	X	X	
HadGEM3-GC31-LL	X	X		X	X	X		X	X		X
INM-CM4-8	X	X	X	X	X	X	X	X	X	X	
INM-CM5-0	X	X	X	X	X	X	X	X	X	X	
IPSL-CM6A-LR	X	X	X	X	X	X	X	X	X	X	
MIROC-ES2L	X	X	X	X	X	X	X	X	X	X	
MIROC6	X	X	X	X	X	X	X	X	X	X	
MPI-ESM1-2-HR	X	X	X	X	X	X	X	X	X	X	
MPI-ESM1-2-LR	X	X	X	X	X	X	X	X	X	X	
MRI-ESM2-0	X	X	X	X	X	X	X	X	X	X	
UKESM1-0-LL	X	X	X	X	X	X	X	X	X		X
									No. of ESM in Ensemble		
Total:	22	21	20	21	22	21	20	21	20 - 22	15	5

mean annual precipitation of the 22 CIMP6 ESM within the 2021–2040 time period (Figure 2), and following the guidance provided by Hausfather *et al.*[64] to exclude "hot models' to approximate the IPCC AR6 averages, 15 ESM were identified to comprise a "Consensus" ensemble which explicitly excluded the hottest models (Table 1). However, as there is still more than a 5% chance for higher ECS models to predict future temperatures[64], a high sensitivity subset of 5 "hot models" was identified to constitute a "High-Risk" ensemble, outlining the potential "risk space" of extreme outcomes. Recent climatic events, however, have also brought these more extreme scenarios more relevant to risk assessment[68].

Four emission scenarios, or CMIP6 Shared Socio-Economic Pathways (SSP)[61,69] are analyzed for each of the 22 ESM, and for each of the two ensembles. However, to simplify the presentation of results, the SSP 5-8.5 for the two ensembles is primarily discussed in the text, with the rationale that global climate is currently worryingly close to tracking this worst-case scenario[70]. However, full results for all four emission scenarios are included in the extended materials, or available upon request. The downscaled ESMs (available from WorldClim.org) were downscaled using the Delta method[71] to 30 arc sec resolution (equivalent to ~1 km^2 at the equator) and using the WorldClim 2.1 historical dataset (1970–2000) as baseline for bias

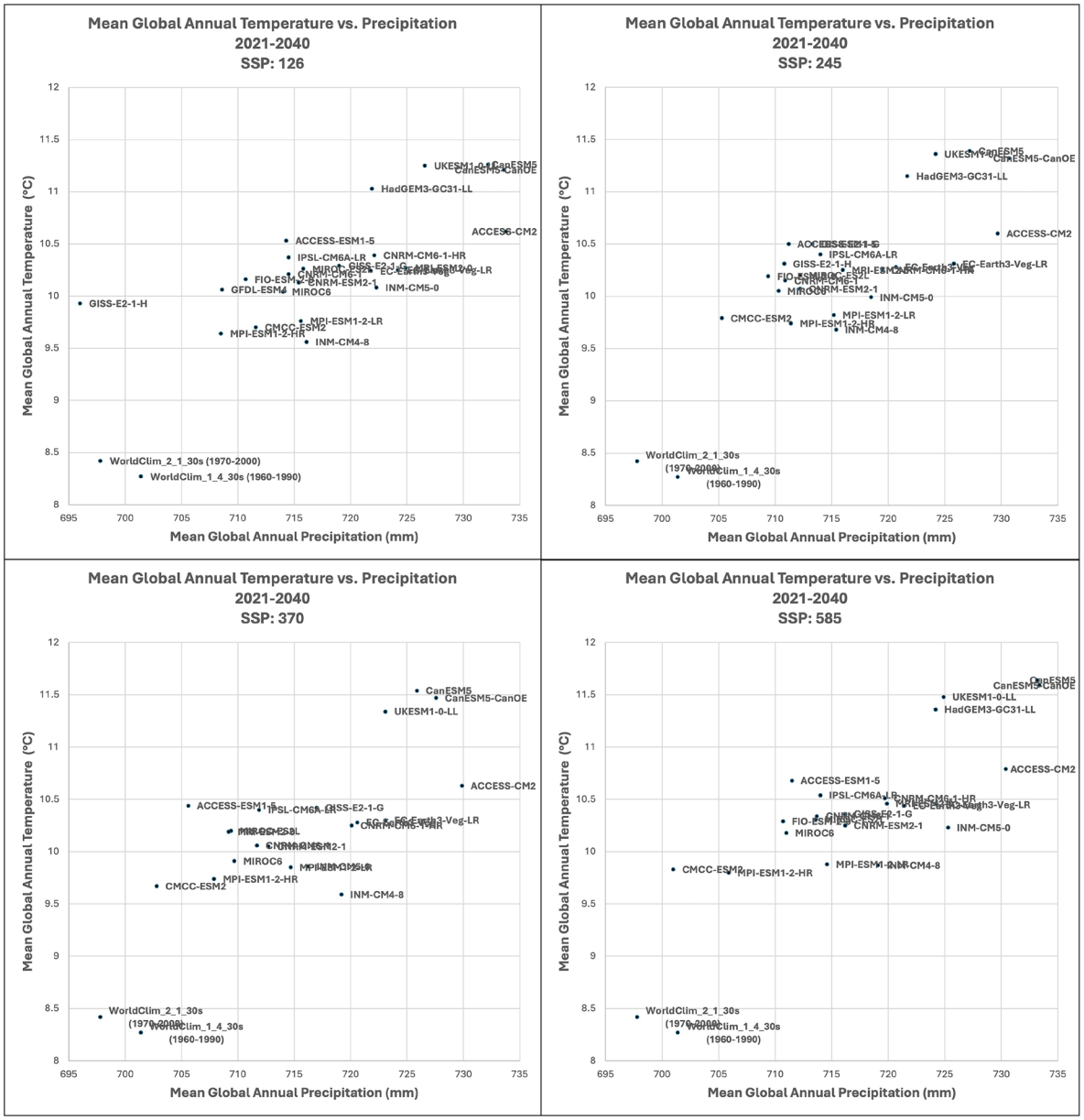


Figure 2. Distribution of 22 CMIP6 Earth System Models along temperature and precipitation gradients (2021–2040). Distribution of average global mean annual temperature and mean annual precipitation of 22 CIMP6 ESM for four shared socio-economic pathways (SSP: 1-26; 2-45; 3-70; 5-85) for the time period 2021–2040.

correction. The Maximum Likelihood Classification[72] algorithm in ArcGIS 10.8[73] was used to construct the projected future spatial distribution of strata, using the modeled future climate conditions as predicted by each of the available CIMP6 ESM and SSP emission scenario combinations (n = 168) for each of the two time periods as input parameters. Selected models within each SSP were combined into a majority ensemble result, using the class with the majority of occurrence within any grid cell as the class for that location. The rate of occurrence of other classes is used as a measure of the uncertainty among models (Table 2). Average uncertainty for strata ranged from 76% to 85%, with an overall average mean uncertainty amongst all ensembles of 81.6%. In general, there was found to be a high level of agreement amongst the ESM included within each of the respective multimodel ensembles as reflected by the Coefficient of Variation of their input variables (Table 3). Agreement was relatively high at the global level for the basic parameters of annual average temperature and annual average precipitation, somewhat less for annual averaged PET and AI, slightly decreasing in the 2041–2060 time period, with significant variability across regions (Figure 3).

Shifting global bioclimatic conditions

Baseline metrics

An overview of the distribution of the global average annual temperature and average annual precipitation projected by the two ensembles, as articulated for each SSP (Figure 4) illustrates that all models indicate global trends of increasing precipitation and increasing temperature in the near-term, more so by the 2041–2060 time period. However, when considering the projected global increase in PET (Figure 5), there emerges a distinct and significant drying trend indicated by decreasing AI values, both in the near-term, and again, more so by 2041–2060. There is, however, significant variability exhibited among regions (Figure 3).

Basic characteristics and key metrics of the 18 EnS Zones, including parameters used in the analysis, are described in Table 4, including their areal distribution, average elevation, several temperature and precipitation metrics, average annual potential evapotranspiration (PET) and aridity index. Cold and Arctic Zones (A- G) generally have lower temperatures, higher elevations, and more significant precipitation in some cases. Likewise, they generally have very high aridity indices, indicating they are less arid, sometimes wet, but this is confounded by many months of temperature below freezing so that PET and plant available moisture are less interpretable, or relevant. Temperate Zones (H- L) have moderate temperatures with varying levels of moisture. The aridity indices here are generally moderate to saturated (1.0) or above, indicating these zones are relatively more humid or mesic (moderately wet). Dry, Arid and Xeric Zones (L,N-Q) are the most arid, characterized by higher temperatures, lower precipitation, higher potential evapotranspiration and low AI values. In general, zones like Extremely Hot and Arid (P) and Extremely Hot and Xeric (Q) are expected to have very dry conditions, while Arctic and Cold zones have lower temperatures and can be both dry or wet.

Shifting areal distribution of bioclimatic zones under climate change scenarios

The areal distribution of the EnS zones is given in Table 5 and Figure 6, reflecting the spatial extent of different homogenous bioclimatic zones across the globe during the baseline period of 1970–2000. Among the large zones, the Extremely Hot and Moist zone has the largest area, covering nearly 20 million km^2, with Extremely Cold and Mesic (F) covering more than15 million km^2 and the Cold and Mesic (G) almost 17 million km^2. The Cool Temperate and Dry (H) zone, covering over 10 million km^2, represents areas with cooler climates but limited precipitation. Warm Temperate and Mesic (K) and Cool Temperate and Moist (H) zones, with areas of 8 million km^2 and

Table 2. Mean Percentage of Agreement Among Earth System Models (ESM) Included Within Each Ensemble. *Mean percentage of agreement among CMIP Phase 6 - Earth System Models (ESM) included within two majority ensembles (Consensus; High Risk), as a measure of uncertainty,* for two time periods (2021–2040; 2041–2060), and two multimodel majority ensembles (Consensus; High-Risk).

Mean Percentage of Agreement						
Year	**Ensemble**	**SSP**				**Average**
		126	**245**	**370**	**585**	
2021–2040	Consensus	83.15	83.72	84.20	82.97	83.51
	High-Risk	85.92	85.23	83.97	84.75	84.97
2021–2040 Average		84.54	84.48	84.09	83.86	84.24
2041–2060	Consensus	78.53	78.20	79.43	77.04	78.30
	High-Risk	83.52	81.22	77.88	76.09	79.68
2041–2060 Average		81.03	79.71	78.66	76.57	78.99
Overall Average		**82.78**	**82.09**	**81.37**	**80.21**	**81.61**

Table 3. Coefficient of Variation of Key Bioclimatic Variables. *Coefficient of Variation (CoV) of key variables among selected datasets within ensembles used as input to the EnS stratification analysis: annual mean temperature (tmean_yr); annual precipitation (prec_yr); annual PET (pet_yr); and Aridity Index,* for two time periods (2021–2040; 2041–2060), and two multi-model majority ensembles (Consensus; High-Risk).

Multi-model Ensemble		Coefficient of Variation (%)			
		2021–2040			
	Scenario	tmean_yr	prec_yr	pet_yr	aridity_index
Consensus	126	1.44	3.64	2.37	4.75
	245	1.44	3.65	2.37	4.83
	370	1.36	3.85	2.33	5.12
	585	1.48	4.31	2.61	5.73
	Ensemble average:	**1.43**	**3.86**	**2.42**	**5.11**
High Risk	126	1.09	2.63	1.71	3.72
	245	1.17	2.68	1.75	3.80
	370	1.30	2.61	1.69	3.58
	585	1.22	2.88	1.71	3.91
	Ensemble average:	**1.20**	**2.70**	**1.72**	**3.75**
Multi-model Ensemble		2041–2060			
	Scenario	tmean_yr	prec_yr	pet_yr	aridity_index
Consensus	126	1.44	3.70	2.41	4.70
	245	1.44	3.82	2.46	4.90
	370	1.36	4.03	2.44	5.19
	585	1.48	4.49	2.71	5.79
	Ensemble average:	**1.43**	**4.01**	**2.51**	**5.15**
High_Risk	126	1.25	3.18	2.17	4.67
	245	1.34	3.47	2.40	5.14
	370	1.72	3.78	2.80	5.66
	585	1.76	4.32	3.04	6.42
	Ensemble average:	**1.52**	**3.69**	**2.60**	**5.47**

2.8 million km^2 respectively, typify temperate regions with conducive temperature and moisture conditions. It represents a significant portion of the Earth's populated surface, generally signifying regions with moderate temperatures and sufficient moisture for vegetation and agricultural production. By comparison, Hot and Extremely Hot regions cover vast areas of the globe, with over 14 million km^2 of Extremely Hot and Xeric (Q) conditions, more than 10 million km^2 of Hot and Dry (N), and nearly 10 million km^2 of Hot and Arid (O). The Hot and Dry/Arid zones are typically found in desert regions, while the Extremely Hot and Moist (R) zone, covering nearly 20 million km^2, is common in tropical rainforests biomes. Extremely Hot and Arid (P) covers a substantial area of over 4 million km^2, primarily in deserts and other dry regions. Arctic (A/B) zones, with about 1.4 million km^2 combined, are much smaller, reflecting the limited extent of these frigid regions which are generally limited to polar regions and high elevations.

Below, as an illustrative example, we provide a summary of key findings reporting the absolute areal changes and percent change for each of the EnS Zones with a comparison from the baseline period (1970–2000) to mid-Century (2041–2060) for both the Consensus and the High-Risk scenarios, as projected under the SSP5 8.5 scenario (full results for all SSPs are given in Table 5).

Summary of projected bioclimatic zone shifts under SSP5–8.5 by mid-century

Projected changes in bioclimatic zone extent under the high-emissions SSP5–8.5 scenario (2041–2060) relative to the historical baseline (1970–2000) reveal substantial spatial redistribution of climatic envelopes. These changes reflect both thermal and hydrological reorganizations of the terrestrial climate space. Below, we summarize each EnS zone's shift in area.

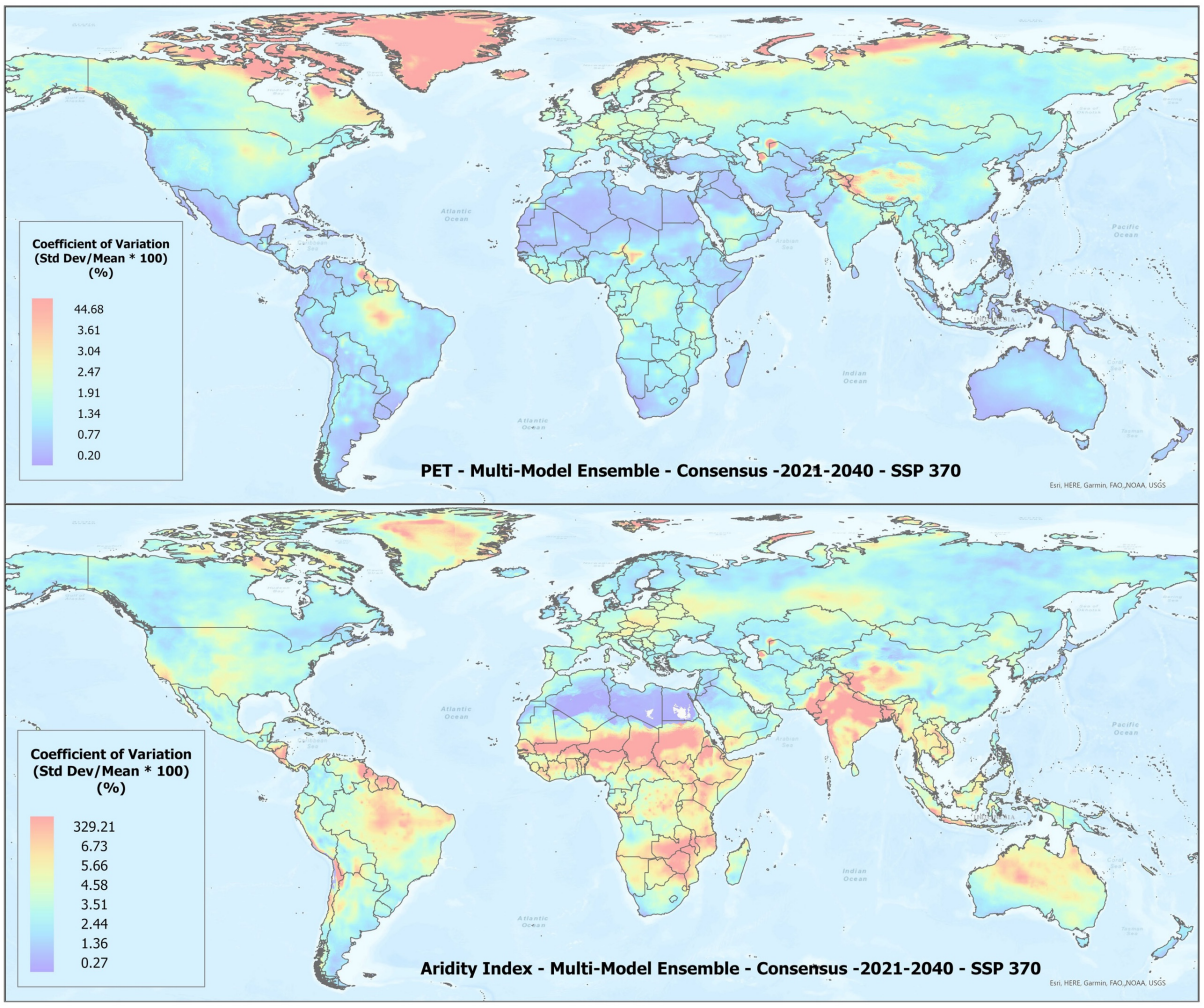


Figure 3. Example of spatial variation of Coefficient of Variation f(CoV) of PET and Aridity Index. Coefficient of variation of PET and Aridity Index of the "Consensus" multimodel majority ensemble for the SPP 370 scenario, shown here to illustrate variation in agreement among the CMIP Phase 6 - Earth System Models (ESM) included within the respective ensemble across the various global regions.

- *Arctic (A)*: This zone represents the coldest and most climatically stable Arctic regions, typically underlain by continuous permafrost. Area is projected to decline from 1,395,834 km^2 to 1,301,659 km^2 under the Consensus model (–6.7%), and to 1,088,848 km^2 under the High-Risk model (–22.0%).The reduction is consistent with observed permafrost degradation and earlier snowmelt at high latitudes.

- *Arctic (B)*: A transitional Arctic zone, typically featuring discontinuous permafrost and tundra-shrub ecotones. Although comprising a relatively very small areal extent, this is projected to expand from 3,107 km^2 to 6,358 km^2 under the Consensus model (+104.6%), and to 29,225 km^2 under the High-Risk model (+840.6%). This dramatic expansion reflects shrub encroachment, and warming-induced northward shifts of boreal ecosystems, and highlights this zone as a sensitive early indicator of Arctic climate response.

- *Extremely Cold and Wet (C):* Found in polar and alpine areas with persistent cold, high precipitation and prolonged snow cover. Area increases from 201,175 km^2 to 261,985 km^2 (+30.2% Consensus) and to 377,385 km^2 (+87.6% High-Risk). Some of these gains may result from upward migration of cold-wet regimes into formerly drier, slightly colder uplands.

- *Extremely Cold and Wet (D):* This zone comprises persistent cold-wet conditions, often found in high montane, glacial margins, or snow-dominated regions with extended snow cover and short growing seasons. Declines from 1,087,896 km^2 to 676,593 km^2 (–37.8% Consensus) and to 619,463 km^2 (–43.1% High-Risk). These reductions are consistent with warming-induced snowline retreat, decreasing snowpack persistence, and reduced cold-season moisture retention.

- *Cold and Wet (E):* Encompasses boreal forests and peat-rich landscapes with long winters and moderate precipitation. Area declines from 959,683 km^2 to 860,979 km^2 (–10.3% Consensus), and to 742,905 km^2 (–22.6% High-Risk). The contraction of areal extent is likely indicative of warming-induced transitions to more mesic or temperate classifications, and

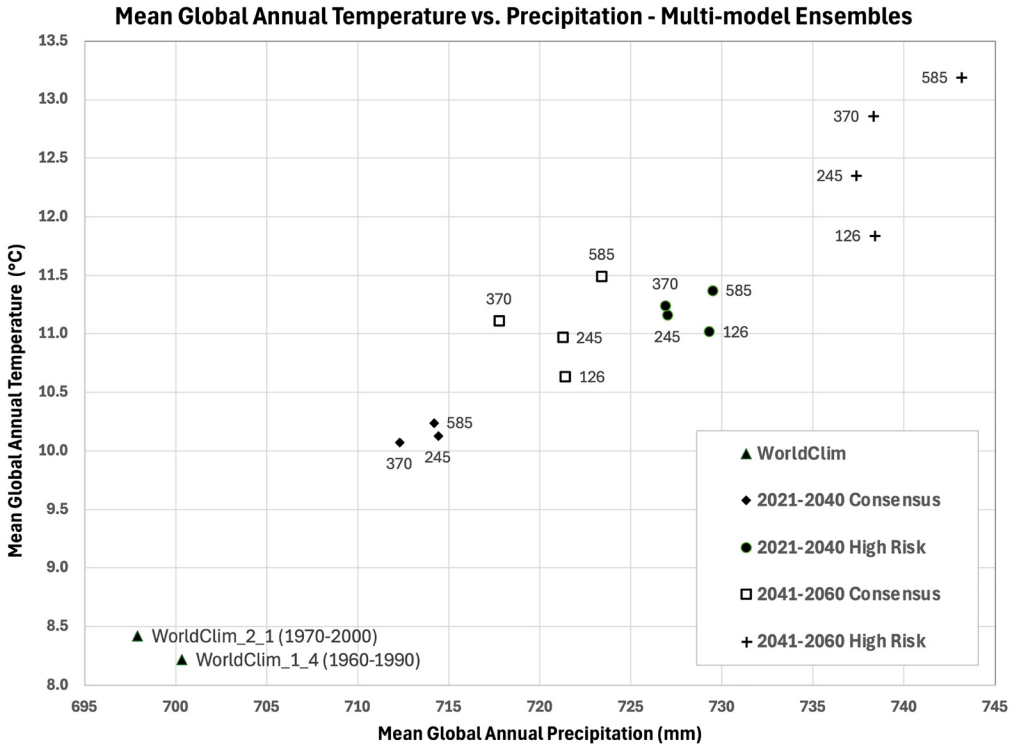


Figure 4. Distribution of historical and projected global averaged annual temperature and annual precipitation. Distribution of historical and projected global averaged annual temperature (°C) and annual precipitation (mm) of two averaged multi-model ensembles, across four shared socio-economic pathways (SSP: 1-26; 2-45; 3-70; 5-85).

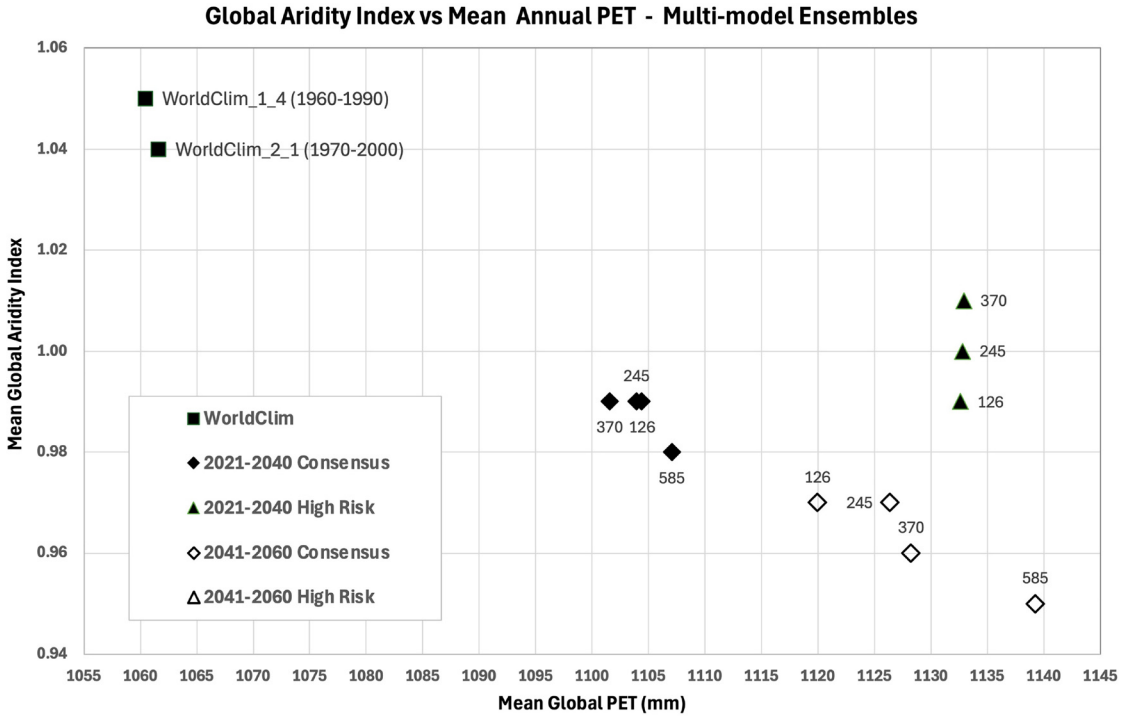


Figure 5. Distribution of historical and projected global averaged PET and Aridity Index. Distribution of historical and projected global averaged PET (mm) and the aridity index (AI) of two averaged multi-model ensembles, across four shared socio-economic pathways (SSP: 1-2.6; 2-4.5; 3-7.0; 5-8.5). Higher AI values indicate wetter conditions, lower values indicate drier conditions.

Table 4. Historical Characteristics of Global EnS Bioclimatic Zones. Historical characteristics of global EnS bioclimatic zones, as per the 1970–2000 (WorldClim v2.1) baseline, including Total Area (km²), Average Elevation (m asl), Mean (tmean_yr), Minimum (tmin_yr), and Maximum (tmax_yr) Annual Temperature (°C), Standard Deviation of the Mean Annual Temperature (tmean_sd ; °C), Annual Precipitation (prec_yr; mm), Potential Evapotranspiration (PET; mm), Standard Deviation of the PET (pet_sd; mm), and the Aridity Index.

Dataset: WorldClim 2.1	Area	Elev	tmean_ yr	tmean_ sd	tmin_ yr	tmax_ yr	tmean_dd	prec_ yr	pet_ yr	pet_ sd	Aridity Index
EnS Zones: 1970–2000	**km²**	**m asl**	**°C**					**mm**			
A. Arctic	1,395,834	2,406	-21.01	9.09	-24.12	-17.90	0	625	76	9	9.86
B. Arctic	3,107	2,221	-9.80	5.99	-13.22	-6.37	6	1516	202	18	7.51
C. Extremely cold and wet	201,175	1,408	-8.54	6.49	-11.42	-5.66	548	1506	228	17	5.96
D. Extremely cold and wet	1,087,896	857	-15.34	10.79	-18.31	-12.36	124	295	148	16	2.08
E. Cold and wet	959,683	816	1.45	5.54	-1.85	4.75	1388	1576	441	29	3.56
F. Extremely cold and mesic	15,175,626	1,169	-9.08	13.24	-13.60	-4.55	889	375	375	35	1.02
G. Cold and mesic	16,925,555	695	-1.24	12.41	-6.70	4.22	1900	539	617	48	0.87
H. Cool temperate and dry	10,134,182	888	4.78	10.78	-1.19	10.76	2868	426	859	55	0.51
I. Cool temperate and xeric	6,729,294	770	9.30	10.83	2.87	15.72	3953	270	1080	63	0.26
J. Cool temperate and moist	2,827,167	574	9.72	6.46	5.00	14.43	3651	1101	873	44	1.30
K. Warm temperate and mesic	8,084,307	822	14.20	6.46	8.42	19.98	5205	931	1199	46	0.80
L. Warm temperate and xeric	5,476,129	728	16.92	6.04	9.88	23.97	6180	374	1462	54	0.26
M. Hot and mesic	9,861,417	681	22.62	2.41	16.81	28.43	8254	1337	1623	24	0.87
N. Hot and dry	10,386,019	753	19.51	4.55	13.10	25.91	7120	834	1538	39	0.57
O. Hot and arid	5,840,002	462	22.41	6.85	15.04	29.77	8185	112	1781	56	0.06
P. Extremely hot and arid	4,675,742	455	25.06	6.22	17.67	32.45	9155	172	1923	50	0.09
Q. Extremely hot and xeric	14,623,764	292	27.58	3.64	20.85	34.31	10071	494	1977	31	0.26
R. Extremely hot and moist	19,976,113	283	25.56	1.17	20.38	30.75	9330	1860	1685	16	1.12

Table 5. Historical Area of EnS Bioclimatic Zones and Percent Change for Two Future Time Periods. Total area of EnS bioclimatic zones (km²) globally for one historical time period (1970–2000) and Percent Change (%) in Total Area for two future projected time periods (2021–2040; 2041–2060), evaluated across four Shared Socio-Economic Pathways (SSP: 1-2.6; 2-4.5; 3-7.0; 5-8.5).

Global Area - EnS Zones (% change)		1970–2000	2021–2040				2041–2060			
Model	SSP:	WC_2.1	126	245	370	585	126	245	370	585
Consensus	Arctic	1,395,834	(3)	(4)	(3)	(4)	(5)	(6)	(6)	(7)
	Arctic	3,107	64	85	76	73	73	82	93	105
	Extremely cold and wet	201,175	10	12	11	15	18	25	24	30
	Extremely cold and wet	1,087,896	(24)	(23)	(21)	(24)	(29)	(32)	(33)	(38)
	Cold and wet	959,683	(7)	(7)	(6)	(8)	(8)	(9)	(10)	(10)
	Extremely cold and mesic	15,175,626	(25)	(25)	(23)	(27)	(33)	(38)	(38)	(45)
	Cold and mesic	16,925,555	(2)	(3)	(2)	(3)	(3)	(3)	(3)	(3)
	Cool temperate and dry	10,134,182	(1)	(0)	(2)	0	(1)	(0)	(2)	(2)
	Cool temperate and xeric	6,729,294	14	14	13	15	16	17	18	21
	Cool temperate and moist	2,827,167	8	9	9	9	10	11	10	9
	Warm temperate and mesic	8,084,307	7	7	6	8	10	11	12	14
	Warm temperate and xeric	5,476,129	(9)	(9)	(10)	(11)	(13)	(17)	(17)	(17)
	Hot and mesic	9,861,417	(14)	(14)	(14)	(16)	(18)	(20)	(22)	(24)
	Hot and dry	10,386,019	(14)	(14)	(15)	(15)	(16)	(19)	(20)	(22)
	Hot and arid	5,840,002	(15)	(14)	(15)	(17)	(20)	(24)	(26)	(31)
	Extremely hot and arid	4,675,742	10	11	12	11	13	14	12	10
	Extremely hot and xeric	14,623,764	44	45	44	49	59	69	75	83
	Extremely hot and moist	19,976,113	2	2	2	2	1	1	(0)	1
High-Risk	Arctic	1,395,834	(9)	(9)	(8)	(10)	(12)	(18)	(21)	(22)
	Arctic	3,107	302	405	481	395	345	514	973	841
	Extremely cold and wet	201,175	22	24	37	30	35	55	96	88
	Extremely cold and wet	1,087,896	(33)	(35)	(34)	(36)	(38)	(36)	(40)	(43)
	Cold and wet	959,683	(7)	(7)	(5)	(8)	(12)	(16)	(16)	(23)
	Extremely cold and mesic	15,175,626	(46)	(46)	(48)	(50)	(55)	(60)	(66)	(69)
	Cold and mesic	16,925,555	2	1	(1)	0	2	(2)	(8)	(11)
	Cool temperate and dry	10,134,182	(2)	(1)	(1)	(2)	(7)	(6)	(3)	(0)
	Cool temperate and xeric	6,729,294	16	17	20	19	17	14	7	2
	Cool temperate and moist	2,827,167	25	23	26	24	28	39	51	60
	Warm temperate and mesic	8,084,307	15	16	17	17	22	26	34	34
	Warm temperate and xeric	5,476,129	(12)	(14)	(12)	(12)	(14)	(13)	(13)	(10)
	Hot and mesic	9,861,417	(19)	(19)	(18)	(19)	(23)	(25)	(25)	(27)
	Hot and dry	10,386,019	(17)	(18)	(18)	(18)	(21)	(23)	(25)	(27)
	Hot and arid	5,840,002	(24)	(25)	(26)	(27)	(30)	(35)	(39)	(42)
	Extremely hot and arid	4,675,742	10	12	11	11	10	5	(2)	(5)
	Extremely hot and xeric	14,623,764	68	70	66	72	79	86	84	86
	Extremely hot and moist	19,976,113	(1)	(1)	2	1	4	8	19	25



Figure 6. Global Area of Ens Zones for One Historical and Two Future Time Periods. Global area (km²) of Ens bioclimatic zones for one historical (Baseline: WC_2.1: 1970-2000) and two future time periods (2021–2040; 2041–2060) showing results for two multi-model majority ensembles: **a.**) Consensus and **b.**) High-Risk.

aligns with observed boreal forest stress and increasing fire activity across high latitudes.

- *Extremely Cold and Mesic (F)*: Comprising dry, cold steppe tundra, and northern boreal / tundra margins with limited precipitation and extended frost periods. Contracts from 15,175,626 km² to 8,392,612 km² (–44.7% Consensus) and to 4,691,945 km² (–69.1% High-Risk). This is a highly impacted zone, reflecting widespread loss of cold continental interiors and high climate sensitivity.

- *Cold and Mesic (G):* Typical of mid-latitude mixed forests and highland temperate grassland, encompassing much of the temperate coniferous belt. such as the northern Rockies, central Asia, and the southern Andes. These systems are climatically transitional, often positioned between boreal and temperate zones, and support a mix of forest types, grazing lands, and temperate biodiversity hotspots. Declines modestly from 16,925,555 km² to 16,424,216 km² (–3.0% Consensus), and more strongly to 15,066,298 km² (–11.0% High-Risk), suggesting encroachment by warmer and drier conditions, potentially

leading to increased vulnerability to fire, pests, and seasonal water stress.

- *Cool Temperate and Dry (H):* Comprised of temperate steppe, semi-arid highland, and includes dry to mesic temperate landscapes with seasonal droughts such as Eurasian steppe zones, Patagonian plains, and semi-arid highland plateaus. Area declines slightly from 10,134,182 km^2 to 9,934,801 km^2 (−2.0% Consensus) and to 10,102,559 km^2 (−0.3% High-Risk). These relatively small shifts suggest near-term climatic stability in many of these continental interiors, but they may mask important and growing exposure to climate extremes, including shifting rainfall patterns and rising temperatures.

- *Cool Temperate and Xeric (I):* Comprised of temperate regions subject to drought and high inter-seasonal variability, low and erratic rainfall, often under strong rain-shadow influence or within continental interiors — such as the Great Plains, western China, or Anatolia. These areas support grazing, irrigated agriculture, and drought-adapted ecosystems. Expands from 6,729,294 km^2 to 8,165,562 km^2 (+21.3% Consensus), and to 6,844,484 km^2 (+1.7% High-Risk). Although substantially less under the High-Risk scenario, this increase may reflect warming-induced aridification and a thermally driven shift into more xeric classifications, with growing seasonal moisture stress and elevated evaporative demand likely to affect both ecosystem function and agricultural potential.

- *Cool Temperate and Moist (J):* Found in humid to sub-humid temperate regions, this zone includes parts of central and northern Europe, the southern Andes, eastern Australia, and the Pacific Northwest of North America. These landscapes support broadleaf and mixed forests and are key zones for both biodiversity and forestry. Increases from 2,827,167 km^2 to 3,070,582 km^2 (+8.6% Consensus), and to 4,514,481 km^2 (+59.7% High-Risk). Expansion may reflect warming in currently colder zones into mesic temperate regimes and becoming more suitable for temperate forest assemblages.

- *Warm Temperate and Mesic (K):* Agriculturally productive regions with generally high land-use intensity, including Mediterranean climatic zones (e.g., southern Europe, California, parts of Chile and South Africa) and moist subtropical highlands (e.g., Ethiopian plateau, southern China, southeastern Brazil). These regions support mixed cropping systems, vineyards, and high-value horticulture, often with seasonal rainfall regimes. Expands from 8,084,307 km^2 to 9,186,018 km^2 (+13.6% Consensus), and to 10,858,638 km^2 (+34.3% High-Risk). This expansion may reflect the poleward and upslope encroachment of warmer, wetter conditions into former temperate zones and drylands, potentially enhancing agricultural suitability in some areas while also increasing exposure to heatwaves, evapotranspiration losses, and seasonal climate variability.

- *Warm Temperate and Xeric (L):* Found in semi-arid Mediterranean and subtropical upland areas characterized by strong interannual rainfall variability and pronounced dry seasons. These regions include parts of the Middle East, southwestern North America, central Asia, and northern Mexico — areas often supporting extensive rangelands or low-input rainfed agriculture. Decreasing from 5,476,129 km^2 to 4,545,379 km^2 (−17.0% Consensus) and to a lesser 4,941,811 km^2 (−9.8% High-Risk), which may reflect bifurcation into either wetter mesic systems (under enhanced seasonal precipitation) or into more arid and xeric classes (under warming and drying scenarios). The instability of this zone underscores its sensitivity to relatively small shifts in temperature and rainfall balance, with implications for agricultural sustainability and water stress.

- *Hot and Mesic (M):* Comprising tropical savannas, monsoon-influenced lowlands, and seasonally wet tropics with pronounced wet-dry cycles — including parts of India, Southeast Asia, northern South America, and sub-Saharan Africa. These areas are highly dynamic, supporting rainfed cropping systems, mixed woodlands, and fire-adapted ecosystems. Decreases from 9,861,417 km^2 to 7,526,648 km^2 (−23.7% Consensus), and to 7,243,885 km^2 (−26.5% High-Risk). The substantial loss suggests increasing aridity and contraction of the savanna-climate envelope, with portions of this zone likely transitioning into xeric or dry forest conditions. This has critical implications for agroecological transitions, biodiversity corridors, and food security in regions dependent on monsoonal reliability. Indicative of moisture stress and encroachment of drier regimes into moist tropics.

- *Hot and Dry (N):* This zone spans dry subtropical belts and marginal arid environments, such as the Kalahari, Thar Desert, and interior Australia, often defined by high temperatures, erratic rainfall, and limited vegetative cover. Many of these areas lie at the climatic threshold between productive rangelands and true deserts. Declines from 10,386,019 km^2 to 8,134,725 km^2 (−21.7% Consensus), and to 7,542,652 km^2 (−27.4% High-Risk). These reductions suggest significant ecological stress and warming-induced aridification, pushing many landscapes past thresholds for productivity or natural vegetation persistence. The contraction may also signal a trajectory into more extreme xeric or hyper-arid states, posing growing challenges for sustainable livelihoods, particularly in semi-arid agrarian zones.

- *Hot and Arid (O*) Typically includes interior deserts and subtropical arid zones with seasonal rainfall, such as the Sahel, Arabian Peninsula, and interior Australia. Contracts from 5,840,002 km^2 to 4,020,916 km^2 (−31.1% Consensus), and to 3,393,073 km^2 (−41.9% High-Risk). These sharp contractions suggest many of these landscapes are exceeding the thermal and moisture thresholds defining aridity, shifting toward hyperarid conditions.

- *Extremely Hot and Arid (P):* This zone encompasses the world's core desert systems — including the Sahara, the Arabian Penisula, and parts of the Iranian Plateau — characterized by extreme temperatures, minimal annual precipitation (<100 mm), and near-total absence of permanent vegetation. Expands from 4,675,742 km^2 to 5,136,913 km^2 (+9.9% Consensus), but slightly contracts to 4,442,277 km^2 (−5.0% High-Risk). These mixed results perhaps suggest that extremely hot and hyper-arid

zones may be undergoing shifts in internal characteristics and boundary definition towards novel bioclimatic conditions, with varying climate sensitivities in this hyper-arid belt.

- *Extremely Hot and Xeric (Q):* This zone includes dryland regions with heat and chronic moisture deficit — increasingly surpassing physiological tolerance thresholds for vegetation. It includes vast swaths of northern Africa, western Asia, interior Australia, and subtropical zones in the Americas. Areal extent of this zone expands dramatically from 14,623,764 km^2 to 26,754,600 km^2 (+83.0% Consensus), and to 27,194,394 km^2 (+86.0% High-Risk). This consistent and extensive bioclimatic shift suggests widespread conversion of hot drylands into ultra-xeric systems with limited productivity and resilience. Such expansion has profound implications for desertification processes, biodiversity loss, climate-driven migration, and the sustainability of marginal agricultural systems under worsening aridity and heat stress.

- *Extremely Hot and Moist (R):* Occupying the hottest and most humid regions on Earth — including the Amazon, Congo Basin, and equatorial Southeast Asia — this zone is defined by high rainfall, persistent humidity, and high potential evapotranspiration. Area increases modestly from 19,976,113 km^2 to 20,235,495 km^2 (+1.3%) under the Consensus model but expands considerably to 24,941,718 km^2 (+24.9%) under the High-Risk model. This projected intensification of hot-humid conditions may signal an expanded spatial extent of equatorial convection zones, with higher temperatures pushing moisture-rich regions beyond historical norms. These shifts could increase climate sensitivity in the tropics, potentially altering cloud dynamics, carbon fluxes, and biodiversity patterns — particularly in systems already close to thermal and hydrological tipping points, and imply an intensification and spatial spread of hot, humid tropical conditions.

Overall, the projections under SSP5–8.5, presented here as an illustrative high-emissions scenario, reveal a pronounced contraction of cooler and wetter bioclimatic zones, including the Arctic, extremely cold and wet, cold and wet, and cold to mesic temperate regions. These losses are especially substantial under the High-Risk ensemble. In contrast, hotter and drier zones, particularly the extremely hot and xeric class, expand dramatically, exhibiting a consistent and extensive bioclimatic shift across both ensemble models. Several transitional and agriculturally critical zones, such as warm temperate mesic areas, show notable expansion, while others (e.g., warm temperate xeric, hot and dry) are reclassified into more extreme categories. While these patterns are broadly consistent, the magnitude of change is greater under the High-Risk projections. These findings illustrate a large-scale redistribution of terrestrial climate space toward hotter and more arid regimes, underscoring the potential impacts of unmitigated climate change on ecological stability, land-use suitability, biodiversity, and the ecosystem services that underpin human well-being.

Latitudinal shifts in bioclimatic zones under climate change scenarios

Analysis of latitudinal shifts in the global EnS bioclimatic zones under future climate projections reveals a clear and measurable poleward migration of bioclimatic zones, with notable variations between hemispheres and between climate model ensembles. Mountain regions were excluded from the analysis, based upon the UNEP-WCMC Mountains of the World[74] dataset, to isolate latitudinal effects from confounding elevational influences, with results clearly demonstrating that climate-driven changes in temperature and precipitation regimes are progressively altering the latitudinal distribution of bioclimatic conditions and terrestrial ecosystems.

In the Northern Hemisphere, bioclimatic zones exhibit a strong and consistent northward shift, with both the Consensus and High-Risk ensembles projecting significant poleward movement (Table 6). The Consensus model found an average latitudinal displacement of +2.75° by 2041–2060, while the High-Risk model estimates a more pronounced shift of +4.96°, with some zones migrating more than +10°. These changes are particularly evident in boreal and temperate biomes, where zones that historically averaged around 55°N now shift toward or beyond 57–60°N. This result is consistent with recent observation[75], and aligns with well-documented ecological shifts in boreal and temperate biomes, where warming temperatures are enabling the expansion of temperate vegetation into traditionally boreal zones. Boreal and tundra ecosystems in Alaska, Siberia, and Fennoscandia are among the fastest-shifting systems, consistent with arctic amplification and rapid warming in these high-latitude continental interiors. These findings are consistent with the observed latitudinal changes in boreal zones[75,76], as observed across Canada, Scandinavia, and northern Eurasia, where satellite data and long-term ecological monitoring indicate northward expansion of temperate vegetation and declines in boreal forest density at their southern margins. supporting evidence of a climate-induced northward migration of these ecosystems[77,78]. Analysis of nearly four decades of satellite data and environmental records reveal that much of the boreal forest has become greener along its northern margins and browner along its southern margins[75].

Similarly, in the Southern Hemisphere, bioclimatic zones are shifting poleward, however, at a more moderate rate compared to the Northern Hemisphere, with the Consensus model averaging +1.66°, and the High-Risk model showing a larger shift of +3.05° southward (Table 6). At least part of this asymmetry in latitudinal migration may be attributed to the greater oceanic influence in the Southern Hemisphere, which moderates temperature fluctuations. Zones typically associated with subtropical drylands and Mediterranean-type ecosystems—such as parts of southern Africa, Australia, and South America—are among those showing moderate to high latitudinal shifts globally. Bioclimatic zones typically associated with subtropical savanna and grassland systems are projected to undergo substantial latitudinal shifts—ranging up to 6–8° under high-emissions scenarios—suggesting significant ecological displacement with profound ecological and socioeconomic implications.

The asymmetry in poleward movement between hemispheres is further highlighted by the distribution of shifts across zones, as illustrated by the violin graph in Figure 7 showing a greater spread in the Northern Hemisphere's latitudinal migration,

Table 6. Average Latitude of Ens Bioclimatic Zones and Change for Two Future Projected Time Periods. Average latitude of EnS bioclimatic zones (decimal degrees; geographic projection) for one historical time period (1970–2000) and change in average latitude (decimal degrees) for two future projected time periods (2021–2040; 2041–2060), a across the four Shared Socioeconomic Pathways (SSP 1-2.6; 2-4.5; 3-7.0; 5-8.5).

Average Latitude - EnS Zones (Decimal Degrees)			Change: Decimal Degrees							
Mountain Regions Excluded		1970–2000	2021–2040				2041–2060			
Ensemble	Northern Hemisphere SSP:	WC_2.1	126	245	370	585	126	245	370	585
Consensus	A. Arctic	74.10	0.67	0.71	0.66	0.76	0.86	0.99	0.95	1.12
	B. Arctic	64.06	(0.46)	0.07	0.22	(0.30)	(0.53)	(0.65)	(0.92)	(0.90)
	C. Extremely cold and wet	66.47	(2.33)	(2.22)	(2.36)	(2.25)	(2.13)	(1.91)	(1.83)	(1.67)
	D. Extremely cold and wet	74.73	0.60	0.55	0.55	0.54	0.55	0.61	0.60	0.60
	E. Cold and wet	58.52	2.28	2.30	2.17	2.39	2.90	3.13	3.27	3.56
	F. Extremely cold and mesic	65.83	1.27	1.28	1.14	1.32	1.77	2.15	2.07	2.69
	G. Cold and mesic	57.04	2.28	2.30	2.12	2.48	2.94	3.25	3.33	3.78
	H. Cool temperate and dry	48.72	3.05	3.08	2.80	3.37	4.00	4.54	4.61	5.29
	I. Cool temperate and xeric	43.46	1.84	1.85	1.76	2.04	2.41	2.69	2.86	3.26
	J. Cool temperate and moist	45.63	2.25	2.35	2.22	2.43	2.72	3.09	3.19	3.67
	K. Warm temperate and mesic	36.87	3.15	3.15	2.87	3.34	3.99	4.37	4.56	5.20
	L. Warm temperate and xeric	34.16	2.52	2.51	2.45	2.69	3.24	3.65	3.89	4.40
	M. Hot and mesic	17.21	4.35	4.32	4.30	4.60	5.56	6.30	6.56	7.37
	N. Hot and dry	29.21	2.03	2.02	1.87	2.15	2.55	2.86	2.97	3.43
	O. Hot and arid	27.78	1.97	1.96	1.90	2.11	2.37	2.64	2.83	3.25
	P. Extremely hot and arid	24.23	2.30	2.30	2.23	2.46	2.82	3.19	3.40	3.88
	Q. Extremely hot and xeric	15.76	0.94	0.93	0.85	1.03	1.37	1.56	1.61	2.01
	R. Extremely hot and moist	8.90	(1.10)	(1.05)	(0.94)	(1.16)	(1.48)	(1.49)	(1.49)	(1.37)
High-Risk	A. Arctic	74.10	0.44	0.50	0.86	0.55	0.61	0.75	1.72	1.27
	B. Arctic	64.06	1.22	1.20	1.78	1.04	1.24	1.85	2.32	2.06
	C. Extremely cold and wet	66.47	(0.26)	(0.42)	(0.48)	0.18	(0.23)	0.47	0.76	1.47
	D. Extremely cold and wet	74.73	1.37	1.34	1.28	1.38	1.48	1.75	1.89	1.92
	E. Cold and wet	58.52	4.46	4.46	4.62	4.60	4.98	5.14	5.12	5.43
	F. Extremely cold and mesic	65.83	3.20	3.21	3.32	3.45	4.24	4.68	5.10	5.53
	G. Cold and mesic	57.04	3.77	3.87	4.05	4.17	4.44	5.01	5.72	6.25
	H. Cool temperate and dry	48.72	4.65	4.83	4.96	5.28	5.70	6.42	7.29	7.96
	I. Cool temperate and xeric	43.46	2.82	2.87	3.03	3.16	3.54	3.80	4.23	4.75
	J. Cool temperate and moist	45.63	3.66	3.89	4.19	4.37	4.90	5.96	6.75	7.15
	K. Warm temperate and mesic	36.87	4.69	4.89	4.95	5.32	5.94	6.78	7.70	8.08
	L. Warm temperate and xeric	34.16	3.55	3.71	3.74	3.98	4.37	4.93	5.64	6.03
	M. Hot and mesic	17.21	5.99	6.40	6.21	6.60	7.57	8.71	9.53	10.45
	N. Hot and dry	29.21	2.99	3.12	3.06	3.34	3.86	4.48	5.34	5.87
	O. Hot and arid	27.78	2.58	2.68	2.63	2.85	3.28	3.79	4.54	5.36
	P. Extremely hot and arid	24.23	3.21	3.23	3.27	3.42	3.82	4.37	5.04	5.35
	Q. Extremely hot and xeric	15.76	1.54	1.57	1.63	1.72	2.15	2.60	3.42	3.72
	R. Extremely hot and moist	8.90	(1.55)	(1.48)	(1.30)	(1.39)	(1.14)	(0.64)	0.21	0.55

Average Latitude - EnS Zones (Decimal Degrees)			Change: Decimal Degrees							
Mountain Regions Excluded		1970–2000	2021–2040				2041–2060			
Ensemble	Southern Hemisphere SSP:	WC_2.1	126	245	370	585	126	245	370	585
Consensus	A. Arctic									
	B. Arctic									
	C. Extremely cold and wet	49.95	(0.01)	(0.00)	(0.00)	(0.02)	(0.03)	(0.08)	(0.10)	(0.11)
	D. Extremely cold and wet	51.50	0.18	0.13	0.27	0.18	0.28	0.38	0.27	0.49
	E. Cold and wet	48.81	0.62	0.65	0.75	0.63	0.79	0.96	1.17	1.37
	F. Extremely cold and mesic	52.25	0.02	0.02	0.02	0.02	0.03	0.19	0.06	(0.07)
	G. Cold and mesic	51.35	0.53	0.56	0.58	0.59	0.61	0.75	0.81	0.84
	H. Cool temperate and dry	46.14	0.65	0.72	0.74	0.82	0.88	1.42	1.67	1.93
	I. Cool temperate and xeric	43.14	1.51	1.63	1.66	1.71	1.87	2.13	2.18	2.25
	J. Cool temperate and moist	42.11	0.85	0.88	0.94	0.93	1.09	1.33	1.49	1.77
	K. Warm temperate and mesic	34.32	1.70	1.72	1.76	1.91	2.38	3.06	3.35	3.70
	L. Warm temperate and xeric	32.01	1.27	1.34	1.35	1.46	1.69	2.12	2.32	2.60
	M. Hot and mesic	16.25	1.50	1.50	1.48	1.67	2.07	2.44	2.63	2.85
	N. Hot and dry	22.57	2.59	2.62	2.60	2.92	3.45	5.00	5.46	6.47
	O. Hot and arid	25.95	1.23	1.31	1.40	1.41	1.64	2.13	2.18	2.40
	P. Extremely hot and arid	21.80	1.30	1.49	1.53	1.57	1.82	2.26	2.40	2.52
	Q. Extremely hot and xeric	14.38	(0.13)	(0.09)	(0.07)	(0.09)	(0.15)	(0.18)	(0.32)	(0.16)
	R. Extremely hot and moist	8.15	0.60	0.59	0.62	0.66	0.65	0.79	0.93	0.99
High-Risk	A. Arctic									
	B. Arctic									
	C. Extremely cold and wet	49.95	(0.09)	(0.08)	(0.09)	(0.08)	(0.18)	(0.24)	(0.29)	(0.37)
	D. Extremely cold and wet	51.50	0.31	0.38	0.42	0.24	0.42	0.71	1.07	1.16
	E. Cold and wet	48.81	1.07	1.13	1.30	1.28	1.38	1.99	2.41	2.60
	F. Extremely cold and mesic	52.25	0.11	0.13	0.11	0.11	0.06	0.25	0.23	0.23
	G. Cold and mesic	51.35	0.78	0.80	0.82	0.83	0.89	1.01	1.12	1.17
	H. Cool temperate and dry	46.14	1.39	1.43	1.47	1.59	2.01	2.80	3.28	3.57
	I. Cool temperate and xeric	43.14	2.21	2.32	2.36	2.39	2.43	2.44	2.49	2.49
	J. Cool temperate and moist	42.11	1.43	1.53	1.59	1.66	2.07	2.89	3.70	4.17
	K. Warm temperate and mesic	34.32	2.99	3.15	3.16	3.35	3.95	4.69	5.25	5.83
	L. Warm temperate and xeric	32.01	1.83	2.00	1.99	2.07	2.47	3.18	3.89	4.32
	M. Hot and mesic	16.25	2.36	2.46	2.46	2.47	2.90	3.65	4.17	5.07
	N. Hot and dry	22.57	4.23	4.51	4.43	4.93	6.22	7.08	7.75	8.24
	O. Hot and arid	25.95	1.78	1.88	1.85	1.91	2.18	2.75	3.33	3.69
	P. Extremely hot and arid	21.80	1.94	2.06	2.02	2.09	2.33	2.64	3.43	3.84
	Q. Extremely hot and xeric	14.38	(0.56)	(0.57)	(0.58)	(0.54)	(0.27)	0.22	0.99	1.29
	R. Extremely hot and moist	8.15	0.81	0.89	0.95	1.00	1.03	1.16	1.35	1.55

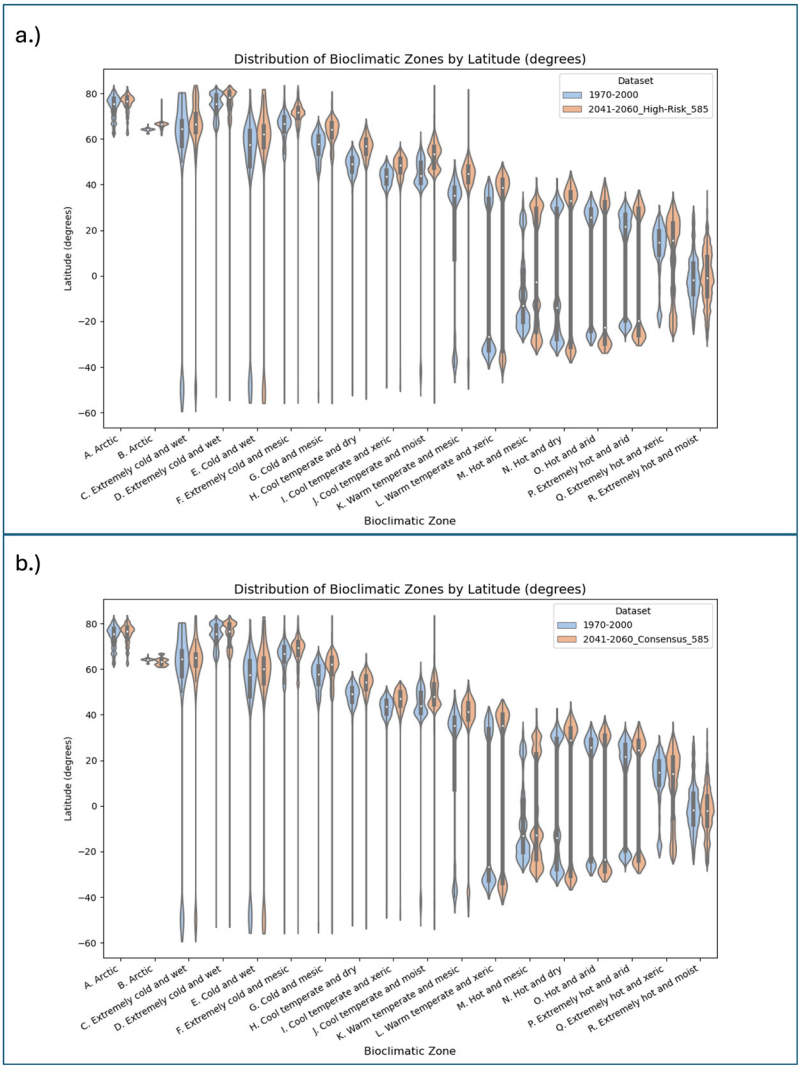


Figure 7. Distribution of EnS Bioclimatic Zones by Latitude. Distribution of EnS bioclimatic zones by latitude (geographic degrees) comparing the historical baseline (WC_2.1; 1970–2000) with the projections for 2041–2060, evaluated for the SSP 5-8.5 scenario for both the **a.**) Consensus multimodel ensemble, and **b.**) High Risk multi-model ensemble.

with some zones exhibiting much faster poleward movement than others. A wider spread at higher latitudes, indicates greater variability in poleward shifts among the different bioclimatic zones, while some zones have a long tail extending farther north, suggesting that certain ecosystems (e.g., boreal forests or tundra) are shifting more rapidly. This difference suggests that regional climate variability is influencing the velocity of bioclimatic shifting, while showing that most zones are exhibiting a steady poleward movement[79,80]. The more constrained latitudinal shifts shown for the Southern Hemisphere reinforce the idea of a moderated response due to oceanic influence. However, certain outliers (long tails) indicate that some specific biomes, such as subtropical drylands or Mediterranean ecosystems, could shift more than others. The uneven distribution of latitudinal shifts in both hemispheres highlight the importance of regional and localized adaptation strategies to account for differential rates of climate-driven ecological change

Altitudinal shifts of mountain bioclimatic zones under climate change scenarios

Bioclimatic zones in mountainous regions (Table 7; Figure 8) are projected to undergo significant upslope migration by mid-century (2041–2060), reflecting well-documented ecological responses to climate warming. This analysis, limited to mountain zones defined by elevation and terrain constraints[74], uses projected changes in mean elevation for each EnS zone from the historical baseline (1970–2000) under both Consensus and High-Risk multi-model ensembles, and shows consistent elevation increases across nearly all zones (Figure 9). Under the Consensus ensemble, average elevation increases for mountain-associated zones range from ~110 m to 340 m. The Extremely Cold and Mesic Zone F, representing high montane tundra and boreal-alpine margins, rises from 2,358 m to 2,699 m, a gain of ~341 m. The Arctic transitional Zone B shifts upward from 1,422 m to 1,869 m (+447 m). These shifts suggest a thermally

Table 7. Average Elevation of Ens Bioclimatic Zones and Change for Two Future Projected Time Periods. Average elevation (m asl) of EnS bioclimatic zones for one historical time period (1970–2000) and change in average latitude (m asl) for two future projected time periods (2021–2040; 2041–2060), evaluated across the four Shared Socioeconomic Pathways (SSP 1-2.6; 2-4.5; 3-7.0; 5-8.5).

Average Elevation: EnS Zones (m asl)			Change Average Elevation (m asl)							
Mountain Regions Excluded		1970–2000	2021–2040				2041–2060			
Ensemble	SSP:	WC_2.1	126	245	370	585	126	245	370	585
Consensus	A. Arctic	2,559	92	98	92	101	104	111	117	125
	B. Arctic	1,422	249	237	241	273	281	341	352	447
	C. Extremely cold and wet	1,108	7	7	8	18	33	57	46	76
	D. Extremely cold and wet	1,485	(206)	(213)	(206)	(229)	(254)	(289)	(287)	(326)
	E. Cold and wet	1,125	(47)	(46)	(45)	(50)	(68)	(76)	(80)	(95)
	F. Extremely cold and mesic	2,358	169	182	153	193	226	279	283	341
	G. Cold and mesic	1,521	66	61	55	71	96	103	101	136
	H. Cool temperate and dry	1,838	70	68	82	68	71	62	73	60
	I. Cool temperate and xeric	1,401	97	97	90	104	157	196	209	251
	J. Cool temperate and moist	1,192	(26)	(35)	(34)	(37)	(38)	(39)	(35)	(24)
	K. Warm temperate and mesic	1,424	42	36	35	43	55	60	56	69
	L. Warm temperate and xeric	1,210	66	66	69	75	92	119	131	150
	M. Hot and mesic	866	124	127	124	135	158	189	198	224
	N. Hot and dry	1,155	42	43	49	47	55	62	68	73
	O. Hot and arid	887	82	82	81	89	112	129	137	161
	P. Extremely hot and arid	762	97	96	95	107	125	137	151	166
	Q. Extremely hot and xeric	586	30	29	31	31	36	43	51	59
	R. Extremely hot and moist	519	85	87	86	97	118	145	158	183
High-Risk	A. Arctic	2,559	142	141	134	141	156	182	183	219
	B. Arctic	1,422	258	258	77	335	346	253	891	885
	C. Extremely cold and wet	1,108	38	34	56	26	32	41	76	71
	D. Extremely cold and wet	1,485	(237)	(243)	(288)	(257)	(305)	(380)	(464)	(438)
	E. Cold and wet	1,125	(74)	(79)	(89)	(73)	(73)	(77)	(88)	(75)
	F. Extremely cold and mesic	2,358	449	471	473	527	591	697	747	871
	G. Cold and mesic	1,521	50	55	66	70	80	130	180	224
	H. Cool temperate and dry	1,838	56	46	58	31	34	(2)	15	(87)
	I. Cool temperate and xeric	1,401	209	221	238	255	311	361	408	439
	J. Cool temperate and moist	1,192	(52)	(49)	(44)	(48)	(22)	(12)	90	22
	K. Warm temperate and mesic	1,424	52	52	53	53	61	71	115	99
	L. Warm temperate and xeric	1,210	109	118	110	121	148	177	202	224
	M. Hot and mesic	866	170	182	180	190	215	244	265	268
	N. Hot and dry	1,155	51	56	54	52	70	86	107	129
	O. Hot and arid	887	124	128	129	137	161	183	191	202
	P. Extremely hot and arid	762	150	152	158	164	173	197	220	228
	Q. Extremely hot and xeric	586	53	52	52	53	67	85	110	125
	R. Extremely hot and moist	519	137	145	143	155	186	218	233	255

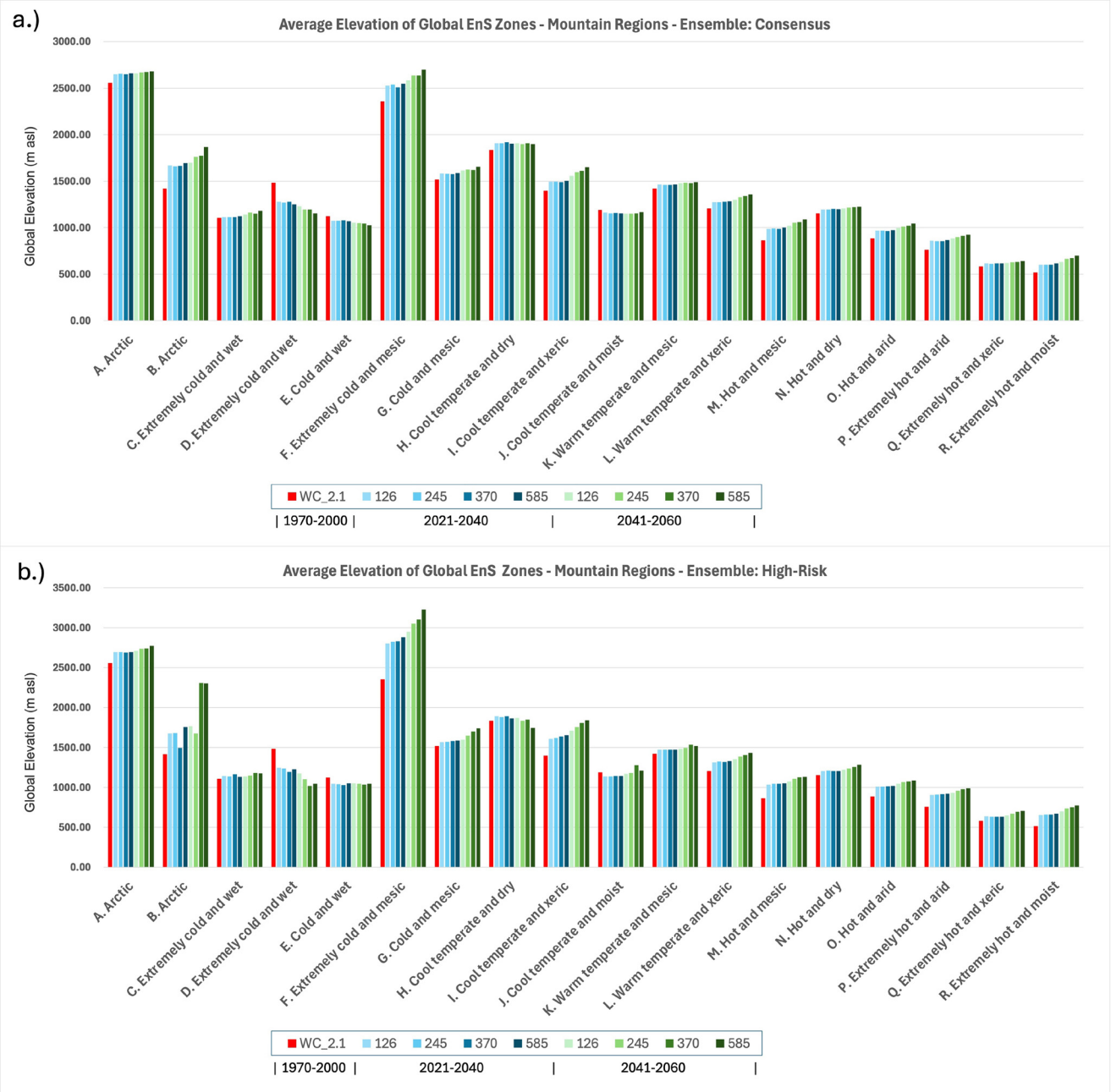


Figure 8. Global Average Elevation of Ens Bioclimatic Zones for One Historical and Two Future Time Periods. Global average elevation of Ens bioclimatic zones for one historical (Baseline: WC_2.1: 1970–2000) and two future time periods (2021–2040; 2041–2060) showing results for two multi-model majority ensembles: **a.**) Consensus and **b.**) High-Risk. Only areas classified as a mountain region[74] are included in this analysis.

equivalent displacement of roughly 2.2–3.0°C, based on a lapse rate of 6.5°C/km, and are consistent with observed responses in montane systems[9,81–85].

Elevational increases are even more pronounced in the High-Risk ensemble, where several zones exhibit vertical displacements exceeding 800 m by mid-century. Arctic Zone B increases to 2,307 m, an upslope migration of ~885 m, while the "Extremely Cold and Mesic" zone reaches over 3,228 m — an increase of ~871 m from its baseline. The "Cool Temperate and Xeric" Zone I, typically found in montane dry forests and steppe uplands, also shifts up by ~439 m. These values highlight the thermal sensitivity of montane ecosystems and point to a strong vertical restructuring of vegetation belts and ecological

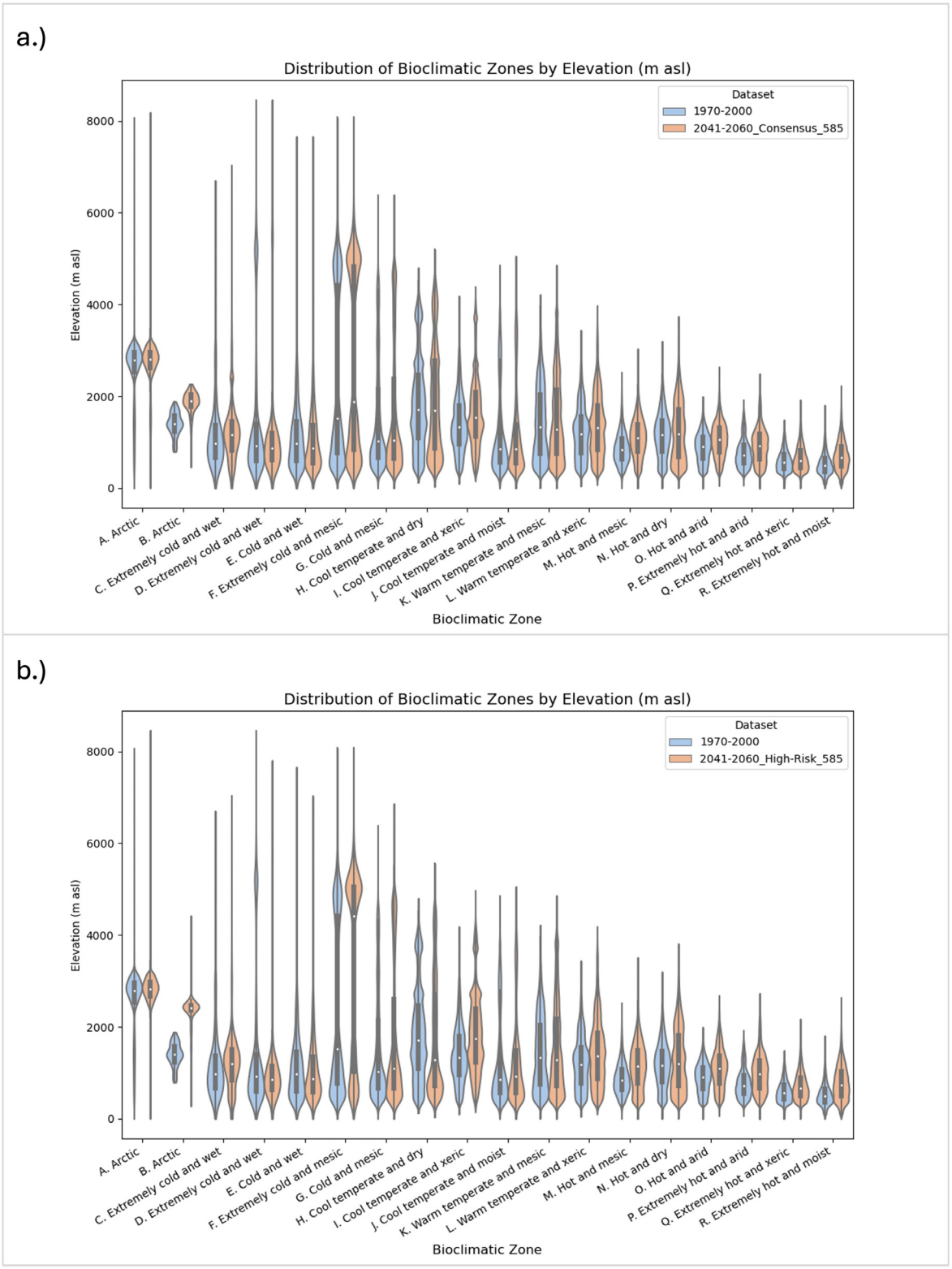


Figure 9. Global Distribution of EnS Bioclimatic Zones by Elevation for One Historical and One Future Time Period. Global Distribution of Ens Zones Bioclimatic Zones by Elevation (m asl) for One Historical and One Future Time Period (2041–2060), showing results for two majority multimodel ensembles: **a.**) Consensus; and **b.**) High-Risk, evaluated for the SSP 5-8.5 scenario. Only areas classified as a mountain region[74] are included in this analysis.

zones. Elevational shifts are among the most rapid and spatially compressed ecological responses to climate change[86–88].

These projected large-scale upslope shifts of bioclimatic zone observed in this study are consistent with empirical studies and modelled projections in key mountainous biodiversity hotspots. For example:

- In the Tropical Andes, elevation gains exceeding 300 m imply substantial displacement of high-elevation endemics[89], where many species are already restricted to narrow elevational bands.
- In the East African Highlands, shifts of 200–270 with steep terrain and limited elevation range exacerbate habitat compression risks[90].
- The Hindu Kush–Himalayan region shows subalpine and alpine belt expansion by ~250 m, altering glacial hydrology, species distribution, and alpine plant communities[91,92].
- The Western Ghats and Eastern Arc Mountains, showing rapid upslope shift (~180–220 m) with limited available elevational range, are globally significant biodiversity refugia with high endemism and are particularly vulnerable to vertical habitat loss[90,93].

Consistent upslope highlight elevational compression, whereby land area diminishes rapidly with altitude, increasing competition for limited habitat and raising extinction risks for montane specialists[81,82,86–88]. In areas such as the Sierra Madre of Central America or Eastern Arc Mountains, the vertical narrowing of suitable climate space is expected to lead to range truncation and loss of high-elevation climate refugia[80,94].

In thermal terms, the magnitude of vertical change observed across mountain regions — often equivalent to 3–5°C of warming — ranks among the most extreme global spatial (ecological) reorganizations, highlighting the vulnerability of mountain ecosystems to global climate change, and foretelling an extended period of biotic and ecosystem perturbation in mountainous regions with potential species decline and extinction[81,82,87,88].

Compositional shifts in bioclimatic zones

Compositional stability refers to the proportion of a bioclimatic zone that retains its original classification over time; conversely, compositional turnover indicates the extent to which a zone's baseline area transitions into other bioclimatic categories due to changing temperature and moisture regimes. Using the EnS WC 2.1 baseline (1970–2000) as the primary reference, comparison with the 2041–2060 projections under the high-emissions SSP5–8.5 scenario reveals distinct and systematic patterns of zonal reorganization (Table 8; Figure 10). Across both the Consensus and High-Risk ensembles, cooler and mesic zones exhibit high rates of internal turnover, while tropical and arid zones show comparatively higher, but still declining, stability (Figure 10).

Under both the Consensus and High-Risk ensembles, cold and montane bioclimatic zones exhibit significant vulnerability to compositional turnover by mid-century under SSP5–8.5 forcing (Figure 11). The Arctic (A) zone, encompassing high-latitude tundra and polar deserts across Siberia, Canada, and Greenland, retains 67% of its original bioclimatic classification under the Consensus model, but drops to 58% under the High-Risk. The Extremely Cold and Wet (C) zone, associated with glaciated coastal regions of Antarctica and alpine snowfields in the Rockies and Alps, retains more than 63% under Consensus and about 51% under High-Risk, indicating accelerated destabilization of snow-dominated landscapes. The Extremely Cold and Wet (D) zone, representative of permanent snow and glacial margins in high-elevation settings like the Andes and the Himalayas, retains just 45% under Consensus and about 36% under High-Risk projections. The Cold and Wet (E) zone, covering boreal forests and subarctic peatlands in Eurasia and North America, retains just over 50% compositional stability under Consensus, declining to 43% under High-Risk, reflecting the progressive transition of these cold-moist systems into warmer or drier classifications. The Extremely Cold and Mesic (F) zone, encompassing cold steppes and tundra margins, is highly unstable, retaining only 18% under Consensus and dropping further to nearly 12% under High-Risk scenarios. These patterns underscore the heightened sensitivity of cold, moisture-dependent systems to climate warming, and suggest that even relatively resilient polar and montane environments face increasing risks of fundamental ecological reorganization as global warming intensifies.

Mid-latitude bioclimatic zones exhibit exceptionally high compositional turnover by mid-century under SSP5–8.5 forcing. The Cool Temperate and Moist (J) zone—covering humid temperate forests in Europe, eastern Asia, and the Pacific Northwest—shows 90.4% turnover under the Consensus model and 96.6% under High-Risk projections. Similarly, the Warm Temperate and Mesic (K) zone, spanning Mediterranean-type ecosystems, moist subtropical highlands, and key agricultural regions such as southern Europe, southern China, and the southeastern United States, records 96.5% turnover under Consensus and 98.8% under High-Risk. These results indicate near-total bioclimatic shifting and turnover across mid-latitude humid zones, with implications for biodiversity, food security, and ecosystem stability[82,95,96]. The loss of climatic stability in these densely populated and highly productive zones poses escalating environmental and socio-economic challenges for global food security, regional sustainability and local livelihoods.

Tropical and arid bioclimatic zones exhibit exceptionally high zonal turnover, which may challenge previous assumptions of their relative resilience. The Extremely Hot and Moist (R) zone, characteristic of humid equatorial lowlands such as the Amazon Basin, Congo Basin, and equatorial Southeast Asia, retains less than 4.8% of its baseline extent under Consensus projections, dropping to just 1.0% under High-Risk scenarios. Similarly, the Hot and Dry (N) zones, encompassing semi-arid regions across southern Africa, interior Australia, and parts of the Indian subcontinent, retain only 2.5% of their baseline

Table 8. Compositional Stability of Historical EnS Bioclimatic Zones. Compositional stability of historical EnS zones (Baseline WC_2.1; 1970–2000), expressed as percent of area (%) globally which shifts to a different EnS zone for two future projected time periods (2021–2040; 2041–2060), evaluated across the four Shared Socioeconomic Pathways (SSP 1-2.6; 2-4.5; 3-7.0; 5-8.5).

Percent of EnS Zone Shifting to Different Zone (%)		2021-2040				2041-2060			
Model	**Baseline: WC_2.1. SSP:**	**126**	**245**	**370**	**585**	**126**	**245**	**370**	**585**
Consensus	A. Arctic	22	23	22	24	26	29	31	33
	B. Arctic	80	70	76	83	90	93	89	94
	C. Extremely cold and wet	27	27	26	28	30	32	33	37
	D. Extremely cold and wet	38	38	35	39	44	48	50	54
	E. Cold and wet	30	31	28	32	36	40	42	46
	F. Extremely cold and mesic	53	53	49	56	65	72	74	82
	G. Cold and mesic	66	67	62	70	79	84	85	90
	H. Cool temperate and dry	78	78	75	81	89	93	93	96
	I. Cool temperate and xeric	78	78	75	83	92	95	97	99
	J. Cool temperate and moist	73	73	70	76	83	86	87	90
	K. Warm temperate and mesic	79	79	76	82	90	93	94	96
	L. Warm temperate and xeric	85	86	86	90	94	99	99	100
	M. Hot and mesic	78	78	78	82	86	89	89	92
	N. Hot and dry	82	82	81	85	91	94	95	98
	O. Hot and arid	100	100	100	100	100	100	100	100
	P. Extremely hot and arid	96	97	97	99	100	100	100	100
	Q. Extremely hot and xeric	53	53	52	56	65	71	73	78
	R. Extremely hot and moist	71	72	71	76	83	91	93	95
High-Risk	A. Arctic	26	25	28	27	31	35	46	42
	B. Arctic	96	98	99	100	99	95	100	92
	C. Extremely cold and wet	36	35	34	34	41	41	43	44
	D. Extremely cold and wet	53	54	62	57	62	65	79	73
	E. Cold and wet	49	50	50	53	59	64	69	73
	F. Extremely cold and mesic	80	81	82	84	89	94	96	97
	G. Cold and mesic	88	89	90	91	93	96	98	99
	H. Cool temperate and dry	94	95	95	96	97	98	99	99
	I. Cool temperate and xeric	97	98	98	99	100	100	100	100
	J. Cool temperate and moist	88	89	90	91	93	95	96	97
	K. Warm temperate and mesic	93	94	94	95	97	98	99	99
	L. Warm temperate and xeric	97	98	97	99	99	100	100	100
	M. Hot and mesic	89	90	90	91	94	95	96	97
	N. Hot and dry	94	95	95	97	98	99	100	100
	O. Hot and arid	100	100	100	100	100	100	100	100
	P. Extremely hot and arid	100	100	100	100	100	100	100	100
	Q. Extremely hot and xeric	71	72	70	73	80	85	89	92
	R. Extremely hot and moist	91	93	93	94	96	96	96	96

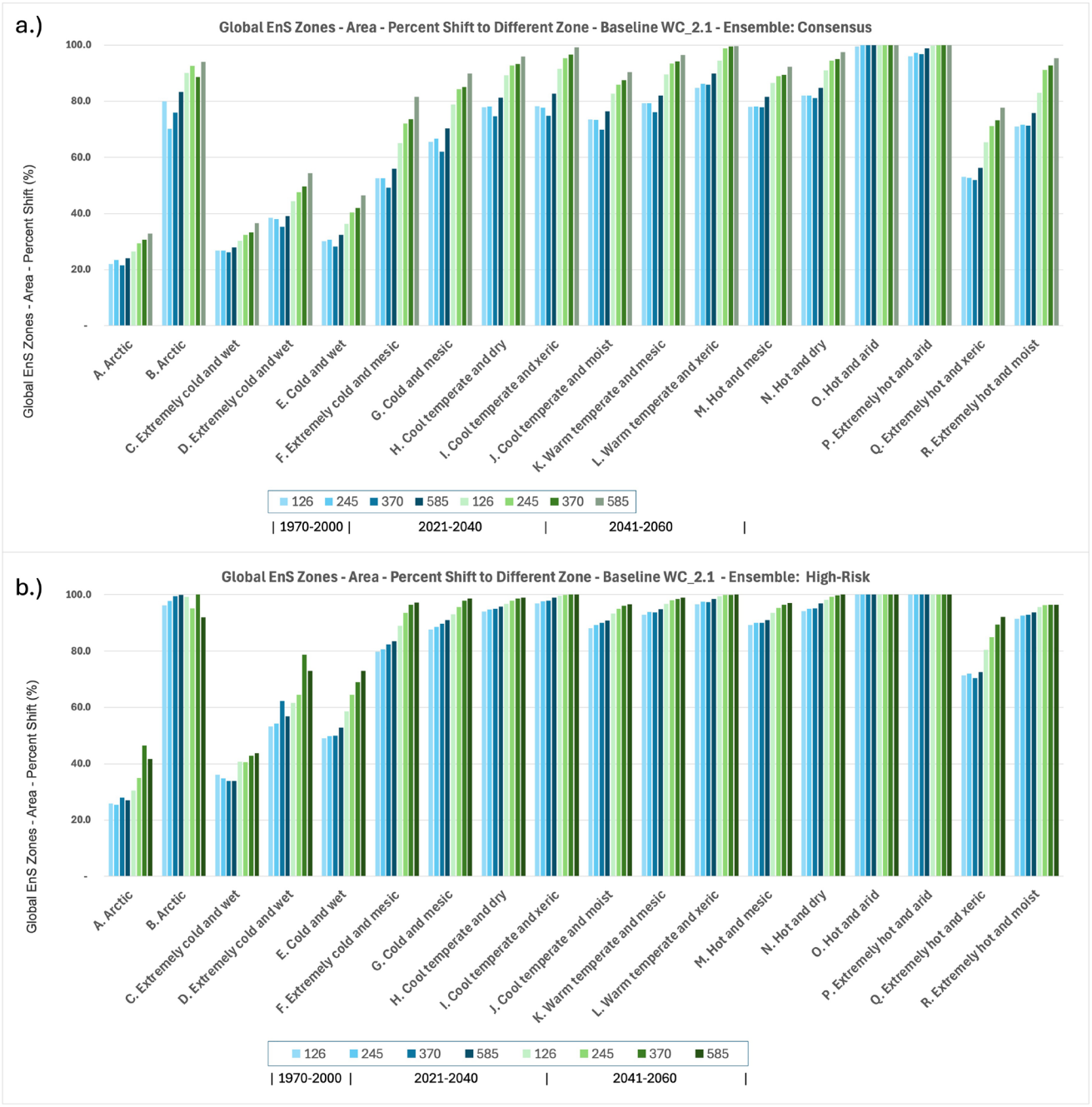


Figure 10. Compositional Shifts of Ens Bioclimatic Zones. Compositional shifts of the EnS bioclimatic zones, globally, showing the area within an EnS zone that shifts to a different EnS zone (Area – Percent Shift (%)), in comparision with the 1970–2000 baseline (WC_2_1), for the Consensus and the High-Risk multi-model ensembles, across four Shared Socio-Economic Pathways (SSP: 1-2.6; 2-4.5; 3-7.0; 5-8.5).

identity under Consensus and are nearly entirely reclassified under the High-Risk ensemble. The Hot and Arid (O) zones, which cover core desert systems such as the Sahara, Arabian Peninsula, and western Australia, experience virtually complete turnover under both model ensembles. These findings indicate that even tropical and subtropical zones, historically considered more compositionally stable due to their climatic extremity, are projected to undergo significant ecological transformation under continued high-emissions trajectories. The results suggest substantial bioclimatic and biotic perturbation of both hot

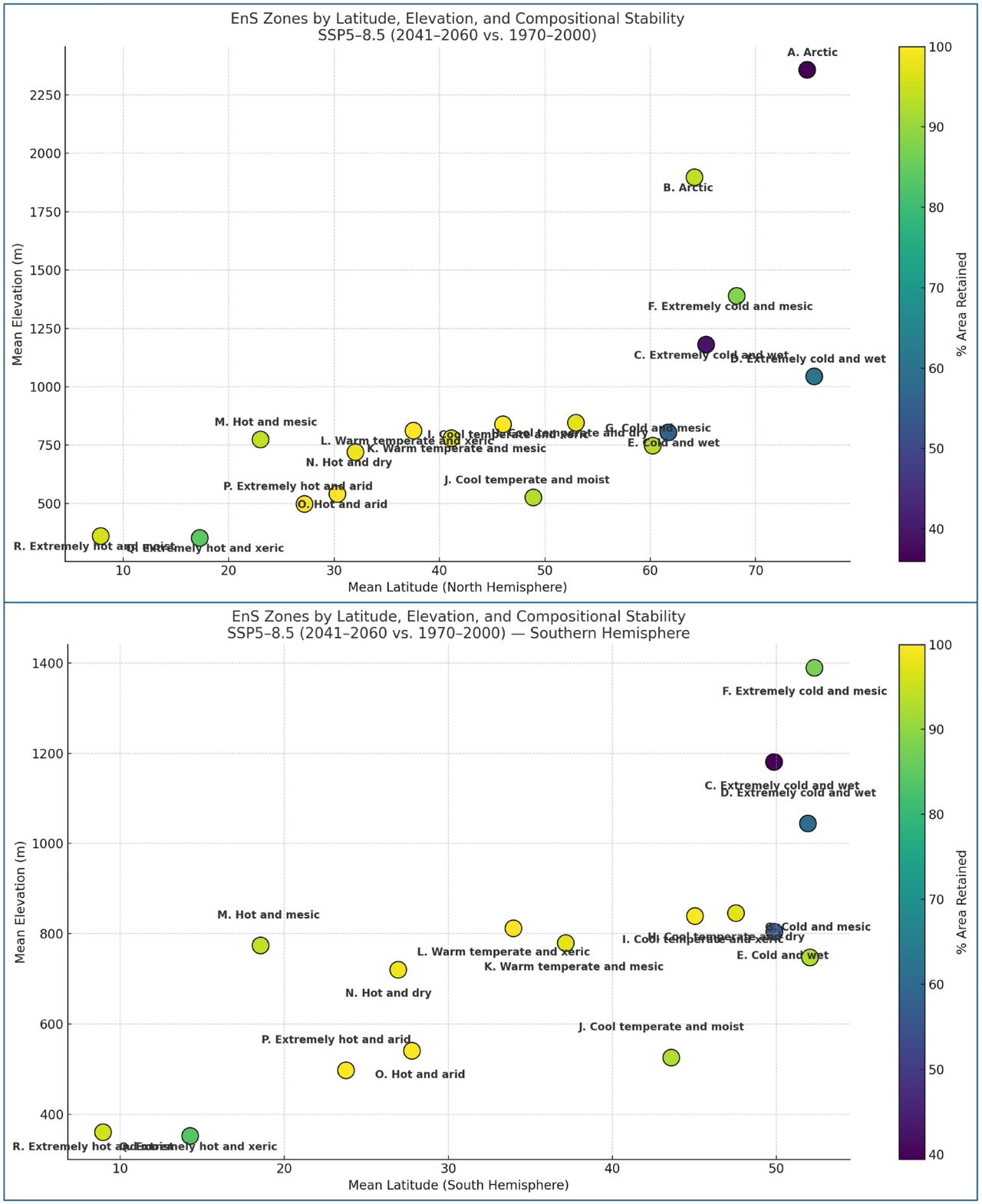


Figure 11. Distribution of EnS Bioclimatic Zones by Latitude, Elevation, and Compositional Stability. Distribution of Ens bioclimatic zones by latitude, elevation, and compositional stability, showing the mean latitude and elevation of the 1970–2000 baseline time period (WC_2.1), and a comparision of the compositional stability (% Area Retained) with the Consensus Ensemble for the Shared Socio-Economic Pathway 8.5 (SSP: 5-8.5), for both the southern and northern hemispheres.

humid, and arid systems globally, with implications for biodiversity persistence, carbon cycling, and regional climate feedbacks[95,97,98].

Discussion

Overview of results

Through application of the EnS framework, this study has produced a high-resolution, globally consistent depiction of how bioclimatic envelopes are shifting across landscapes and across the globe. Our results show clear trends: contraction of cooler and mesic zones, poleward and upslope migration of many mid-latitude zones, and expansion of hotter and more arid conditions. Compositional analyses show relatively higher zonal stability in tropical and subtropical regions, but high vulnerability and turnover in temperate, montane, and high-latitude systems. The projected shifting of the bioclimatic envelopes and associated microclimatic and ecological niches, and in some cases stochastic non-contiguous movement of bioclimatic conditions across landscapes, continents, and the globe, will have, and is having, profound ecological and socioeconomic implications. The compositional and elevational shifts, and the more general poleward migration of bioclimatic zones evident from the analysis suggest an extended period of bioclimatic, ecological and biotic perturbation[80], with widespread impacts for ecosystem functioning and on the provision of ecosystem services across all continents and biomes. These projected rapid transitions to locally novel bioclimatic conditions will impact not only on natural ecosystems, wildlife and wildlife habitat, plant communities, species distributions, and pollinator synchronization, but also, notably, cause the displacement or suitability of current agriculturally suitable zones, particularly in temperate regions, as well as areas suitable for human habitation. Tropical regions may become increasingly difficult for human activities, especially for those working outside[99] or other vulnerable populations, with implications for economic productivity. Taken together, the results of the global analysis and the projected trends and observed patterns confirm we are currently in a profound period of ecological perturbance and fundamental reorganization of the Earth's bioclimatic zones in response to global climate forcing. The ensemble results highlight both the magnitude of expected changes and the variability across space and models—critical information for forecasting ecosystem transitions and delineating future potential risk space, guiding conservation priorities, and developing regional sustainable development and climate adaptation strategies.

This study presents global results (at the EnS "zone" level) to illustrate the general geographical applicability and the "big picture" insight that can be had at the global scale with the EnS methodology, as well as demonstrating the general utility of the resultant EnS database of CMIP6 future projections. However, the relatively high spatial resolution of this dataset, applied at the finer scales of the "EnS "strata" (as opposed to zonal) level, allows (with some care given for increased local uncertainly) the application of this methodology to more defined, specific regional and local geographical contexts, and/or focused on specific thematic areas of interest. While the global analysis illustrates the power of the EnS methodology to integrate and interpret climate projections, in this case the CMIP6 ESM, in more ecologically and easily interpretable terms, this capacity for interpretive insight is specifically more evident at the regional to local levels, where bioclimatic homologues may be easily recognized and intuitively understood by stakeholders, policymakers, and the public.

The regional variability and local nature of bioclimatic strata and their associated biotically relevant trends underscore the need for regional, local, and adaptive land management strategies (and communication) to mitigate the impacts of rapidly shifting bioclimatic envelopes and environmental regimes. The spatially explicit results produced by this framework (at 30 arc seconds resolution) are well suited for national and sub-national adaptation planning, conservation prioritization, and climate-smart agriculture applications. While the variability between climate models and scenarios further emphasizes the spatial and temporal heterogeneity and uncertainty of modeled and projected change, much of the results reported in this study align with documented trends from empirical sources suggesting the EnS projections as ecologically realistic and empirically corroborated, at least in terms of trends, if not magnitude.

Correspondence with observed trends and empirical change

The spatial and compositional transitions identified through the EnS framework correspond strongly with empirical observations of climate-driven ecological change, offering support for the framework's predictive and diagnostic robustness. Multiple independent datasets and monitoring networks have documented latitudinal and elevational shifts in species distributions, ecosystem boundaries, and vegetation dynamics that mirror the projected shifting and reorganization of EnS zones. Upslope migration of alpine plant communities in the European Alps, Tropical Andes, and Himalayas have been documented with observed mean elevational shifts of ~0.3–0.5 m/year[75,88,100,101]. While these rates are notably lower than the ~2.0–5.8 m/year upslope averaged velocity projected for mountain EnS zones (200–300 meters by mid-century), the directional alignment supports the idea that high-elevation ecosystems are already undergoing climate-driven reorganization and responding to shifting bioclimatic conditions, and the potential lag with species' ability to move and adapt. MODIS-based vegetation productivity indices show greening trends in high-latitude ecosystems (e.g., tundra and boreal forest transition zones) indicative of warming-induced northward expansion[75], while thermal degradation of permafrost and drying of peatlands are consistent with compositional shifts in the "Cold and Mesic" and "Cold and Wet" EnS zones. The high spatial resolution of the EnS CMIP6 ensembles (and the datasets in the *Future_Global_Ens Database*) reveal fine-scale variation that aligns with observed sub-regional trends, for example, the compression of upper-montane habitats and expansion of subtropical drylands in East Africa and South Asia.

In contrast to the extensive compositional turnover projected for temperate and cold bioclimatic zones, tropical and arid systems exhibit somewhat greater internal inertia under future climate scenarios. Nevertheless, substantial internal

reorganization and zonal shifting is projected across tropical forests biomes, semi-arid regions, and desert systems, suggesting that these ecosystems, long considered climatically more resilient, are increasingly vulnerable to intensified warming and hydrological stress. These findings align with the traditional perception of tropical and arid zones as ecologically stable under climate change, up to a point, highlighting that even regions already characterized by thermal or moisture extremes are susceptible to significant internal transformation[13,30]. Observed patterns of forest degradation, desert expansion, and altered precipitation regimes in tropical and subtropical regions further reinforce the likelihood of profound future shifts[98]. The emerging evidence suggests that while tropical and arid systems may resist complete zonal reclassification longer than temperate and montane ecosystems, they are nevertheless highly vulnerable to the destabilizing effects of continued global warming[5,13,30].

The EnS methodology has demonstrated high internal accuracy when reconstructed from climate inputs, with kappa statistics exceeding 0.916 and user accuracy above 91% in comparison with the original GEnS dataset[10,102]. Comparative studies using alternative classification methods—such as Random Forests or neural networks—have shown similar spatial patterns but lower overall agreement with established bioclimatic boundaries[11]. EnS also shows strong structural concordance with other ecological zonation frameworks, including Köppen-Geiger classifications and WWF terrestrial ecoregions[12,103], while offering the advantage of being statistically derived and ecologically interpretable[8]. The availability of two historical time periods offers a opportunity to "ground truth" observed climate change over a recent decade: zones known to be experiencing ecological transitions (e.g., the Tibetan Plateau, the Canadian boreal belt, and the Eastern Himalayas) exhibit high compositional turnover, showing the EnS abilituy to monitor real-world change.

Elevational displacement: observed trends and modeled velocity

The EnS ensemble analysis projects significant upslope displacement of mountain bioclimatic zones under future climate scenarios, with modeled elevation gains of 110–180 meters under the majority ensemble and 250–320 meters under the high-risk ensemble by mid-century (2041–2060). These values correspond to an annual elevational velocity of ~2.0–3.3 m/year (Consensus) and 4.5–5.8 m/year (High-Risk). These rates substantially exceed observed biological responses, such as those documented by the GLORIA network, which has tracked alpine plant communities shifting ~2–5 meters per decade (~0.3–0.5 m/year) across mountain systems including the European Alps, Tropical Andes, and Himalayas[88,100]. Similar lags have been reported in avian and insect communities in the East African Highlands, where species richness and composition are changing more slowly than underlying climate envelopes, and in the Hindu Kush-Himalaya, where upslope tree line movement averages less than 2.6 meters per year[104] over recent decades.

This discrepancy highlights the difference between the rapid movement of bioclimatic conditions and the lagged response of ecological communities due to dispersal limitations, geo-ecolgoical constraints, and biotic interactions[80,83,88,94,105,106]. EnS zone shifts reflect changes in climate suitability, providing an early-warning signal of where ecosystems may undergo future restructuring, even if biotic responses are not yet evident. The projected rapid upslope velocity of EnS elevation change underscores the vulnerability of topographically constrained systems[94], especially in regions with steep gradients and limited habitat availability at higher elevations, such as the Eastern Arc Mountains, Central American Highlands, and many other mountain regions. In these cases, upward compression of EnS zones exacerbates risks of habitat loss and extinction[107], particularly for endemic and range-restricted species[80,94].

Both observed and projected results point to increased ecological risk with delayed mitigation and underscore the urgent need for climate- and elevation-informed conservation strategies, notably:

- **Preservation of altitudinal corridors** to facilitate species movement along elevation gradients,
- **Protection of upper slope refugia and montane transition zones**, which act as critical buffers for biodiversity under warming scenarios,
- **Climate-aware restoration planning** for degraded mountain systems, prioritizing future climate suitability and connectivity,
- **Monitoring and early-warning systems** to track shifts in vegetation zones and species range margins in real-time,
- **Incorporation of elevational dynamics into protected area design**, ensuring that conservation boundaries accommodate future upslope movement,
- **Community-based adaptation strategies** in montane landscapes, recognizing the dependency of upland communities on climate-sensitive ecosystems such as cloud forests and montane grasslands.

Utility of environmental stratification for climate-resilient planning

The results presented here illustrate the power of environmental stratification to convert climate model outputs into actionable ecological insights. By combining high spatial resolution with interpretable and ecologically meaningful bioclimatic strata (and the GEnS taxonomy), EnS enables detailed analysis of bioclimatic change at scales relevant to decision-making, allowing for both global assessments and regional to locally specific applications. For instance, the identification of high-risk zones with low compositional stability or high spatial turnover provides direct inputs for prioritizing conservation efforts, land-use planning, and food security. Zones such as "Cold and Wet" and "Cool Temperate and Moist," which show >50% transition rates in some regions, could serve as focal areas for various forms of resilience-building, habitat restoration, or assisted migration strategies. Essentially, all of the EnS bioclimatic

strata (n=125) and all regions of the globe are undergoing rapid change, at various rates, and can benefit from an improved understanding of the direction and magnitude of that change. By focusing on statistically and bioclimatically coherent spatial units, EnS avoids many of the limitations associated with raw climate variables or broad biome models, offering enhanced interpretability for policy and practice. By providing baselines and quantifying the spatial rate at which ecologically relevant bioclimatic conditions are shifting, EnS provides a metric with utility for environmental and biodiversity conservation, informing the design of biodiversity corridors, climate refugia, assisted migration strategies in mountain regions where climate tracking failure is likely[80,83,108], as well as local adaptation, rural landuse, and urban planning. Importantly, in terms of food security, the type of results provided by this analysis are of great utility for developing agricultural sustainability and resilience, plant breeding for future conditions, habitat restoration, and species selection for agroforestry[47,109] or other long-rotation tree or forestry plantations.

Applications across sectors: conservation, agriculture, and sustainable development

The implications of shifting EnS zones, although not specifically analyzed or articulated in this global study, span multiple sectors critical to sustainability. In conservation, for example, environmental stratification can identify regions of high vulnerability, ecological novelty, or future refugia, guiding the design of effective protected area networks and prioritizing areas for habitat connectivity and species migration corridors[18,20]. Likewise, for the agricultural sector, understanding future bioclimatic conditions will be essential to inform plant breeding, climate-smart farming systems, crop suitability assessments, and ensure food security as landscape change accelerates[22,110,111]. As an example, results highlight particularly rapid zonal transitions in montane East Africa and the Himalayan foothills, regions where smallholder systems are highly sensitive to climate variability and food security is already an issue. For supporting sustainable development, adaptation and strategic planning, the EnS methodology enables the delineation of both future climate and "climate risk spaces" that delineate ecological vulnerabilities, helping target adaptation efforts, and identify regions where transformative adaptation will be required[28]. An interpretable understanding of shifting bioclimatic conditions is required to inform effective Nature-based Solutions (NbS) and ecosystem-based adaptation (EbA) strategies, providing spatially explicit baselines for monitoring how changing conditions might impact the provisioning of ecosystem services that underpin resilience in both human and natural systems[25,26].

From global to local: a framework for regionalization

While this study provides a global overview, the greatest utility of the EnS methodology lies in its regional and local application. Because the EnS framework is scale independent, it can be applied to any climate dataset or spatial extent, including at national and subnational scales, enabling local decision-makersto assess climate risks and opportunities with spatial specificity. Downscaling and customizing the methodology to local environmental gradients and policy contexts enhances relevance for regional land-use planning, adaptation financing, agricultural zoning, and biodiversity offsets. High-resolution regional EnS analyses have already demonstrated utility in areas such as Southeast Asia[12,17,20,47], the Hindu-Kush Himalayas[17,47,103,109,112], and Central Asia[113,114], but more widespread adoption would improve integration of current and future rapidly changing bioclimatic conditions across global frameworks, e.g., the SDGs, UNFCCC National Adaptation Plans (NAPs), and the Post-2020 Global Biodiversity Framework[115].

Future directions and integration with emerging technologies

Advances in earth observation and remote sensing technologies, AI-driven ecological modeling, and big data analytics offer opportunities for enhancing and applying the EnS framework. Coupling environmental stratification with predictive modeling and monitoring of ecosystem responses (e.g., vegetation phenology, land degradation, species shifts) can provide or improve early warning systems. Integration with socio-economic datasets also enables deeper analysis of coupled social-ecological systems under climate stress[18]. The EnS framework is well-positioned to serve as a bridge between climate science and decision-making, especially when combined with participatory and interdisciplinary approaches to adaptation planning. As the availability and quality of high-resolution geospatial earth observation, climate and other datasets advance and become more generally accessible, the opportunity to combine this methodology using a set of improved data inputs with advanced geospatial analysis (e.g. artificial intelligence classification methods incorporating a greater range of inputs) will allow for more topically relevant questions and more targeted results in the future.

Conclusion

The Environmental Stratification (EnS) methodology offers a powerful, scalable, and ecologically realistic framework for interpreting the complex spatial patterns of climate change. By integrating key climatic variables into discrete, interpretable bioclimatic zones, EnS transforms raw model outputs into ecologically meaningful insights that are accessible to researchers, practitioners, policymakers, and the general public. This study demonstrates that EnS methodology is capable of revealing both broad-scale global patterns, such as the poleward and upslope migration of climate zones, and fine-grained regional changes that are directly relevant to local adaptation planning. The framework not only reveals the magnitude and direction of projected shifts but also identifies zones of high turnover and relative stability, offering critical guidance for prioritizing conservation and land management efforts.

What distinguishes EnS from other climate classification approaches is its flexibility and interpretability. It functions effectively across spatial scales and climate model ensembles, making it well-suited for scenario-based planning. Its outputs can be used to assess climate risk exposure, ecological vulnerability, and land-use suitability under current and future conditions. The compositional and spatial analyses enabled by EnS have particular utility for climate-sensitive sectors such as agriculture, forestry, biodiversity conservation, and sustainable development. Because it integrates ecological processes and environmental

gradients intuitively, EnS facilitates communication with local stakeholders and decision-makers, bridging the often-wide gap between complex climate data and actionable planning tools.

The utility of environmental stratification methodologies, and the EnS framework in particular, will increase with the increased availability of higher resolution spatial and temporal data, and as climate adaptation and mitigation become more urgent and more spatially targeted. The purely statistically based approach of the EnS methodology allows integration of new earth observation and remote sensing data products, real-time monitoring systems, and socio-economic datasets, enabling deeper insight into coupled human-natural systems. By providing a common ecological language across scales—from global assessments to community-level planning—EnS can serve as a foundational tool for anticipating ecological transitions, identifying opportunity spaces for adaptation, and supporting transformative resilience strategies in the face of rapid climate change.

Ethics and consent

Ethical approval and consent were not required.

Data availability

The *Future_Global_EnS Database* is archived and available online under a CC-BY 4.0 license on the Open Research Europe Repository, hosted by Zenodo at this link: https://doi.org/10.5281/zenodo.15099763[116].

The database contains the main results of the global geospatial modeling of projected climate change impacts on the geographic distribution and shifting of bioclimatic strata, as described here in this article, and provides a set of high-resolution (30 arc-seconds) global raster datasets of bioclimatic zones and strata produced using the EnS methodology. This release includes reconstructions of current and future global EnS for:

- Two historical periods:
  - 1960–1990 (WorldClim 1.4), 1970–2000 (WorldClim 2.1)
- Two future periods: 2021–2040, 2041–2060
  - 22 CMIP6 Earth System Models (ESMs)
- Four emission scenarios (SSPs):
  - SSP1-2.6, SSP2-4.5, SSP3-7.0, SSP5-8.5
- Two multi-model averaged ensembles:
  - Consensus Ensemble (15 ESMs, excluding high ECS models)
  - High-Risk Ensemble (5 “hot” models projecting extreme climate outcomes)

The EnS data layers have been processed for distribution online as Geo-TIFFs. Supplementary tables and figures are available online on the Figshare Data Repository as “Extended Data: CMIP6-Based Global Estimates of Future Aridity Index and Potential Evapotranspiration for 2021–2060” at https://doi.org/10.6084/m9.figshare.26095363 (Zomer *et al.*, 2024). These are available under a CC-BY 4.0 license in one file containing supplementary tables and a figure including:

- Global Mean Annual Climatic Parameters for All Included CMIP_6 ESM
- Mean Annual Climatic Parameters for all Multi-model Ensembles by Region
- Coefficient of Variation for all Multi-model Ensembles by Region
- Map of Global Regions used in the Regional Analysis

Code availability

The algorithms used to conduct the EnS analysis was coded in Python 3.2 and uses the ArcPy (ArcGIS) package. They are available under a Apache 2.0 license on Figshare at this link below:

https://doi.org/10.6084/m9.figshare.28715036.v1

The main Python coded scripts used in the analysis and available online include:

- Calculate Variables
- Signature Analysis
- ESM - Classify
- Multimodel Ensemble - Classify
- Multimodel Ensemble – Uncertainty

Software availability

Source code available from: https://github.com/rzomer/Future_Global_EnS_Algorithm_Python_Code

MIT license

Copyright: © 2025 Zomer *et al.* This is an open access work distributed under the terms of the Creative Commons Attribution License, which permits unrestricted use, distribution, and reproduction in any medium, provided the original work is properly cited.

Acknowledgements

The authors gratefully acknowledge the CMCC Foundation, the University of Sassari, the Center for Mountain Futures, Kunming Institute of Botany, and the Chinese Academy of Sciences Presidential Fellowship program for hosting, supporting, and facilitating this effort. We would very much thank and

acknowledge the EU Open Research Repository for hosting, archiving, and providing access to the Future_Global_EnS Database. We acknowledge and thank the World Climate Research Programme, which, through its Working Group on Coupled Modelling, coordinated and promoted CMIP6. We thank the climate modeling groups for producing and making available their model output, the Earth System Grid Federation (ESGF) for archiving the data and providing access, and the multiple funding agencies who support CMIP6 and ESGF. We also thank Robert Hijmans and WorldClim.org for providing the high resolution downscaled CMIP6 Future Projections and the historical WorldClim datasets.

References

1. Calvin K, *et al.*: **IPCC, 2023: Climate Change 2023: synthesis report, summary for policymakers**. Contribution of Working Groups I, II and III to the Sixth Assessment Report of the Intergovernmental Panel on Climate Change [Core Writing Team, H. Lee and J. Romero (eds.)]. IPCC, Geneva, Switzerland, 2023; 1–34.
Reference Source
2. Hansen JE, Sato M, Simons L, *et al.*: **Global warming in the pipeline.** *Oxf Open Clim Chang.* 2023; **3**(1): kgad008.
Publisher Full Text
3. Blunden J, Boyer T: **State of the climate in 2023.** *Bull Am Meteorol Soc.* 2024; **105**: S1–S484.
Reference Source
4. Steffen W, Rockström J, Richardson K, *et al.*: **Trajectories of the earth system in the anthropocene.** *Proc Natl Acad Sci U S A.* 2018; **115**(33): 8252–8259.
PubMed Abstract | **Publisher Full Text** | **Free Full Text**
5. Grimm NB, Chapin FS, Bierwagen B, *et al.*: **The impacts of climate change on ecosystem structure and function.** *Front Ecol Environ.* 2013; **11**(9): 474–482.
Publisher Full Text
6. Scheffers BR, De Meester L, Bridge TCL, *et al.*: **The broad footprint of climate change from genes to biomes to people.** *Science.* 2016; **354**(6313): aaf7671.
PubMed Abstract | **Publisher Full Text**
7. Matthews T, Raymond C, Foster J, *et al.*: **Mortality impacts of the most extreme heat events.** *Nat Rev Earth Environ.* 2025; **6**: 193–210.
Publisher Full Text
8. Metzger MJ, Brus DJ, Bunce RGH, *et al.*: **Environmental stratifications as the basis for national, European and global ecological monitoring.** *Ecol Indic.* 2013; **33**: 26–35.
Publisher Full Text
9. Zomer RJ, Trabucco A, Wang M, *et al.*: **Environmental stratification to model climate change impacts on biodiversity and rubber production in Xishuangbanna, Yunnan, China.** *Biol Conserv.* 2014; **170**: 264–273.
Publisher Full Text
10. Metzger MJ, Bunce RGH, Jongman RHG, *et al.*: **A high-resolution bioclimate map of the world: a unifying framework for global biodiversity research and monitoring.** *Glob Ecol Biogeogr.* 2013; **22**(5): 630–638.
Publisher Full Text
11. Soteriades AD, Murray-Rust D, Trabucco A, *et al.*: **Understanding global climate change scenarios through bioclimate stratification.** *Environ Res Lett.* 2017; **12**(8): 084002.
Publisher Full Text
12. Johnston JM, Zomer RJ, Wang M: **Predicting future vegetated landscapes under climate change: application of the Environmental Stratification methodology to protected areas in the lower mekong basin.** *Ecosystem-Based Management, Ecosystem Services and Aquatic Biodiversity.* 2020; 561–580.
Publisher Full Text
13. Elsen PR, Saxon EC, Simmons BA, *et al.*: **Accelerated shifts in terrestrial life zones under rapid climate change.** *Glob Chang Biol.* 2022; **28**(3): 918–935.
PubMed Abstract | **Publisher Full Text**
14. Metzger MJ, Bunce RGH, van Eupen M, *et al.*: **An assessment of long term ecosystem research activities across European socio-ecological gradients.** *J Environ Manage.* 2010; **91**(6): 1357–1365.
PubMed Abstract | **Publisher Full Text**
15. Villoslada M, Bunce RGH, Sepp K, *et al.*: **A framework for habitat monitoring and climate change modelling: construction and validation of the Environmental Stratification of Estonia.** *Reg Environ Change.* 2016; **17**: 335–349.
Publisher Full Text
16. Kyker-Snowman E, Lombardozzi DL, Bonan GB, *et al.*: **Increasing the spatial and temporal impact of ecological research: a roadmap for integrating a novel terrestrial process into an earth system model.** *Glob Chang Biol.* 2022; **28**(2): 665–684.
PubMed Abstract | **Publisher Full Text** | **Free Full Text**
17. Zomer RJ, Trabucco A, Metzger MJ, *et al.*: **Projected climate change impacts on spatial distribution of bioclimatic zones and ecoregions within the Kailash Sacred Landscape of China, India, Nepal.** *Clim Change.* 2014; **125**: 445–460.
Publisher Full Text
18. Hossain MS, Basak SM, Amin MN, *et al.*: **Social-ecological systems approach for adaptation to climate change.** *Sustain Dev.* 2024; **32**(3): 2766–2778.
Publisher Full Text
19. Siders AR, Pierce AL: **Deciding how to make climate change adaptation decisions.** *Curr Opin Environ Sustain.* 2021; **52**: 1–8.
Publisher Full Text
20. Zomer RJ, Xu J, Wang M, *et al.*: **Projected impact of climate change on the effectiveness of the existing protected area network for biodiversity conservation within Yunnan Province, China.** *Biol Conserv.* 2015; **184**: 335–345.
Publisher Full Text
21. YEPD: **Yunnan Biodiversity Strategy Action Plan - Five Year Priority Action Plan**. 2014.
22. Rosenzweig C, Tubiello FN: **Adaptation and mitigation strategies in agriculture: an analysis of potential synergies.** *Mitig Adapt Strat Glob Chang.* 2007; **12**(5): 855–873.
Publisher Full Text
23. Cui RY, Waldhoff S, Clarke L, *et al.*: **Evaluating the regional risks to food availability and access from land-based climate policies in an integrated assessment model.** *Environ Syst Decis.* 2022; **42**(4): 547–555.
PubMed Abstract | **Publisher Full Text** | **Free Full Text**
24. Trancoso R, Syktus J, Allan RP, *et al.*: **Significantly wetter or drier future conditions for one to two thirds of the world's population.** *Nat Commun.* 2024; **15**(1): 483.
PubMed Abstract | **Publisher Full Text** | **Free Full Text**
25. Ellis PW, Page AM, Wood S, *et al.*: **The principles of natural climate solutions.** *Nat Commun.* 2024; **15**(1): 547.
PubMed Abstract | **Publisher Full Text** | **Free Full Text**
26. Bossio DA, Cook-Patton SC, Ellis PW, *et al.*: **The role of soil carbon in natural climate solutions.** *Nat Sustain.* 2020; **3**: 391–398.
Publisher Full Text
27. Sandi SG, Rodriguez JF, Saintilan N, *et al.*: **Resilience to drought of dryland wetlands threatened by climate change.** *Sci Rep.* 2020; **10**(1): 13232.
PubMed Abstract | **Publisher Full Text** | **Free Full Text**
28. Fedele G, Donatti CI, Harvey CA, *et al.*: **Limited use of transformative adaptation in response to social-ecological shifts driven by climate change.** *Ecol Soc.* 2020; **25**(1): 25.
Publisher Full Text
29. Sparey M, Cox P, Williamson MS: **Bioclimatic change as a function of global warming from CMIP6 climate projections.** *Biogeosciences.* 2023; **20**(2): 451–488.
Publisher Full Text
30. Bonannella C, Hengl T, Parente L, *et al.*: **Biomes of the world under climate change scenarios: increasing aridity and higher temperatures lead to significant shifts in natural vegetation.** *PeerJ.* 2023; **11**: e15593.
PubMed Abstract | **Publisher Full Text** | **Free Full Text**
31. Beck HE, Zimmermann NE, McVicar TR, *et al.*: **Present and future Köppen-Geiger climate classification maps at 1-km resolution.** *Sci Data.* 2018; **5**: 180214.
PubMed Abstract | **Publisher Full Text** | **Free Full Text**
32. Mawdsley JR, O'Malley R, Ojima DS: **A Review of climate-change adaptation strategies for wildlife management and biodiversity conservation.** *Conserv Biol.* 2009; **23**(5): 1080–1089.
PubMed Abstract | **Publisher Full Text**
33. Blenckner T, Ammar Y, Müller-Karulis B, *et al.*: **The risk for novel and disappearing environmental conditions in the Baltic Sea.** *Front Mar Sci.* 2021; **8**: 745722.
Publisher Full Text
34. González-Pérez A, Álvarez-Esteban R, Penas Á, *et al.*: **Bioclimatic**

characterisation of specific native Californian Pinales and their future suitability under climate change. *Plants (Basel).* 2023; **12**(10): 1966.
PubMed Abstract | Publisher Full Text | Free Full Text

35. Wang S, Liu F, Zhou Q, *et al.*: **Simulation and estimation of future ecological risk on the Qinghai-Tibet Plateau.** *Sci Rep.* 2021; **11**(1): 17603.
PubMed Abstract | Publisher Full Text | Free Full Text

36. Jongman RHG, Bunce RGH, Metzger MJ, *et al.*: **Objectives and applications of a statistical environmental stratification of Europe.** *Landsc Ecol.* 2006; **21**: 409–419.
Publisher Full Text

37. Beckmann M, Didenko G, Bullock JM, *et al.*: **Archetypes of agri-environmental potential: a multi-scale typology for spatial stratification and upscaling in Europe.** *Environ Res Lett.* 2022; **17**(11): 115008.
Publisher Full Text

38. Sayre RJ, Dangermond J, Frye C, *et al.*: **A new map of global Ecological Land Units — An ecophysiographic stratification approach.** 2014; 46.
Publisher Full Text

39. Strobl M: **Alexander Von Humboldt's climatological writings.** *Ger Life Lett.* 2021; **74**(3): 371–393.
Publisher Full Text

40. Koppen W: **Die Klimate Der Erde.** Walter de Gruyter, 1923.
Publisher Full Text

41. Troll C: **Karte der Jahreszeiten-Klimate der Erde.** *Erdkunde.* 1964; **18**(1): 5–28.
Publisher Full Text

42. Reddy SJ: **Agroclimatic classification of the semi-arid tropics I. A method for the computation of classificatory variables.** *Agricultural Meteorology.* 1983; **30**(3): 185–200.
Publisher Full Text

43. Landsberg HE, Lippmann H, Paffen K, *et al.*: **Weltkarten zur Klimakunde / World maps of climatology.** 1965; 19–25.
Publisher Full Text

44. Metzger MJ, Brus DJ, Bunce RGH, *et al.*: **Environmental stratifications as the basis for national, European and global ecological monitoring.** *Ecol Indic.* 2013; **33**: 26–35.
Publisher Full Text

45. Ortega M, Metzger MJ, Bunce RGH, *et al.*: **The potential for integration of environmental data from regional stratifications into a European monitoring framework.** *J Environ Plan Manag.* 2012; **55**(1): 39–57.
Publisher Full Text

46. Metzger MJ: **The global environmental stratification: a high-resolution bioclimate map of the world.** [dataset] *The University of Edinburgh.* 2018.
Publisher Full Text

47. Ranjitkar S, Sujakhu NM, Merz J, *et al.*: **Suitability analysis and projected climate change impact on Banana and Coffee production zones in Nepal.** *PLoS One.* 2016; **11**(9): e0163916.
PubMed Abstract | Publisher Full Text | Free Full Text

48. Zomer RJ, Trabucco A, Metzger M, *et al.*: **Environmental stratification of Kailash sacred landscape and projected climate change impacts on ecosystems and productivity: ICIMOD Working Paper 2013/1.** International Centre for Integrated Mountain Development (ICIMOD), 2013.
Reference Source

49. Cooper DM, Dugmore AJ, Kitchener AC, *et al.*: **A kingdom in decline: holocene range contraction of the lion (*Panthera leo*) modelled with global environmental stratification.** *PeerJ.* 2021; **9**: e10504.
PubMed Abstract | Publisher Full Text | Free Full Text

50. Fick SE, Hijmans RJ: **WorldClim 2: new 1-km spatial resolution climate surfaces for global land areas.** *Int J Climatol.* 2017; **37**(12): 4302–4315.
Publisher Full Text

51. Metzger MJ, Schröter D, Leemans R, *et al.*: **A spatially explicit and quantitative vulnerability assessment of ecosystem service change in Europe.** *Reg Environ Change.* 2008; **8**: 91–107.
Publisher Full Text

52. Metzger M, Bunce R, Jongman RHG, *et al.*: **A climatic stratification of the environment of Europe.** *Glob Ecol Biogeogr.* 2005; **14**(6): 549–563.
Publisher Full Text

53. Hijmans RJ, Cameron SE, Parra JL, *et al.*: **Very high resolution interpolated climate surfaces for global land areas.** *Int J Climatol.* 2005; **25**(15): 1965–1978.
Publisher Full Text

54. Zomer RJ, Trabucco A: **Global aridity index and potential evapotranspiration (ET0) database v3 (Global_AI_PET_v3)**. 2022.
Publisher Full Text

55. Zomer RJ, Trabucco A: **Future global aridity index and PET database (CIMP_6)**. Science Data Bank. 2024.
Publisher Full Text

56. Melnick RL, Jarvis L, Hendley P, *et al.*: **GEnZ explorer: a tool for visualizing agroclimate to inform research and regulatory risk assessment.** *Transgenic Res.* 2023; **32**(4): 321–337.
PubMed Abstract | Publisher Full Text | Free Full Text

57. Tou JT, Gonzalez RC: **Pattern recognition principles.** *ZAMM J Appl Math Mech Z für Angew Math Mech.* 1974; **57**: 353–354.

58. Ball GH, Hall DJ: **ISODATA, A novel method of data analysis and pattern classification**. Stanford Research Institute, 1965.
Reference Source

59. Erbek FS, Özkan C, Taberner M: **Comparison of maximum likelihood classification method with supervised artificial neural network algorithms for land use activities.** *Int J Remote Sens.* 2004; **25**(9): 1733–1748.
Publisher Full Text

60. Rodriguez-Galiano VF, Ghimire B, Rogan J, *et al.*: **An assessment of the effectiveness of a random forest classifier for land-cover classification.** *ISPRS J Photogramm Remote Sens.* 2012; **67**: 93–104.
Publisher Full Text

61. Eyring V, Bony S, Meehl GA, *et al.*: **Overview of the Coupled Model Intercomparison Project Phase 6 (CMIP6) experimental design and organization.** *Geosci Model Dev.* 2016; **9**(5): 1937–1958.
Publisher Full Text

62. Mora C, Frazier AG, Longman RJ, *et al.*: **The projected timing of climate departure from recent variability.** *Nature.* 2013; **502**(7470): 183–187.
PubMed Abstract | Publisher Full Text

63. IPCC: **Climate change 2014: synthesis report. Contribution of working groups I, II and III to the fifth assessment report of the intergovernmental panel on climate change**. IPCC, Geneva, Switzerland, 2015.

64. Hausfather Z, Marvel K, Schmidt GA, *et al.*: **Climate simulations: recognize the 'hot model' problem.** *Nature.* 2022; **605**(7908): 26–29.
PubMed Abstract | Publisher Full Text

65. Kikstra JS, Nicholls ZRJ, Smith CJ, *et al.*: **The IPCC sixth assessment report WGIII climate assessment of mitigation pathways: from emissions to global temperatures.** *Geosci Model Dev.* 2022; **15**(24): 9075–9109.
Publisher Full Text

66. Smith, *et al.*: **The earth's energy budget, climate feedback sand climate sensitivity: supplementary material.** In: *Climate change 2021: the physical science basis. Contribution of working group I to the sixth assessment report of the intergovernmental panel on climate change*. (eds. Masson-Delmotte *et al.*) 2021.
Reference Source

67. Scafetta N: **CMIP6 GCM validation based on ECS and TCR ranking for 21st century temperature projections and risk assessment.** *Atmosphere.* 2023; **14**(2): 345.
Publisher Full Text

68. Trust S, *et al.*: **Climate Scorpion – the sting is in the tail**. The Institute and Faculty of Actuaries and University of Exeter, 2024.
Reference Source

69. O'Neill BC, Tebaldi C, van Vuuren DP, *et al.*: **The Scenario Model Intercomparison Project (ScenarioMIP) for CMIP6.** *Geosci Model Dev.* 2016; **9**(9): 3461–3482.
Publisher Full Text

70. World Meteorological Organization: **State of the global climate 2024**. World Meteorological Organization, Geneva, Switzerland, 2025.
Reference Source

71. Ramirez J, Jarvis A: **Downscaling global circulation model outputs**. CIAT, 2010.
Reference Source

72. Richards JA, Jia X: **Remote sensing digital image analysis: an introduction**. (4th Ed.). Springer, 2006.
Reference Source

73. ESRI: **How maximum likelihood classification works**. 2025.
Reference Source

74. UNEP-WCMC: **Mountains of the world**. 2000.
Reference Source

75. Berner LT, Goetz SJ: **Satellite observations document trends consistent with a boreal forest biome shift.** *Glob Chang Biol.* 2022; **28**(10): 3275–3292.
PubMed Abstract | Publisher Full Text | Free Full Text

76. Montesano PM, Frost M, Li J, *et al.*: **A shift in transitional forests of the North American boreal will persist through 2100.** *Commun Earth Environ.* 2024; **5**(1): 290.
PubMed Abstract | Publisher Full Text | Free Full Text

77. Chagnon C, Moreau G, D'Orangeville L, *et al.*: **Strong latitudinal gradient in temperature-growth coupling near the treeline of the Canadian subarctic forest.** *Front For Glob Chang.* 2023; **6**: 1181653.
Publisher Full Text

78. Rotbarth R, van Nes EH, Scheffer M, *et al.*: **Boreal forests are heading for an open state.** *Proc Natl Acad Sci U S A.* 2025; **122**(2): e2404391121.
PubMed Abstract | Publisher Full Text | Free Full Text

79. VanDerWal J, Murphy HT, Kutt AS, *et al.*: **Focus on poleward shifts in species' distribution underestimates the fingerprint of climate change.** *Nat Clim Change.* 2013; **3**: 239–243.
Publisher Full Text

80. La Sorte FA, Jetz W: **Tracking of climatic niche boundaries under recent climate change.** *J Anim Ecol.* 2012; **81**(4): 914–925.
PubMed Abstract | Publisher Full Text

81. Freeman BG, Scholer MN, Ruiz-Gutierrez V, *et al.*: **Climate change causes upslope shifts and mountaintop extirpations in a tropical bird community.** *Proc Natl Acad Sci U S A.* 2018; **115**(47): 11982–11987.
PubMed Abstract | Publisher Full Text | Free Full Text

82. Freeman BG, Lee-Yaw JA, Sunday JM, *et al.*: **Expanding, shifting and shrinking: the impact of global warming on species' elevational distributions.** *Glob Ecol Biogeogr.* 2018; **27**(11): 1268–1276.
Publisher Full Text

83. Chan WP, Lenoir J, Mai GS, *et al.*: **Climate velocities and species tracking in**

global mountain regions. *Nature.* 2024; **629**(8010): 114–120.
PubMed Abstract | Publisher Full Text | Free Full Text

84. Chen IC, Hill JK, Ohlemüller R, *et al.*: **Rapid range shifts of species associated with high levels of climate warming.** *Science.* 2011; **333**(6045): 1024–1026.
PubMed Abstract | Publisher Full Text

85. Diffenbaugh NS, Field CB: **Changes in ecologically critical terrestrial climate conditions.** *Science.* 2013; **341**(6145): 486–492.
PubMed Abstract | Publisher Full Text

86. Rumpf SB, Hülber K, Klonner G, *et al.*: **Range dynamics of mountain plants decrease with elevation.** *Proc Natl Acad Sci U S A.* 2018; **115**(8): 1848–1853.
PubMed Abstract | Publisher Full Text | Free Full Text

87. Dullinger S, Gattringer A, Thuiller W, *et al.*: **Extinction debt of high-mountain plants under twenty-first-century climate change.** *Nat Clim Chang.* 2012; **2**: 619–622.
Publisher Full Text

88. Steinbauer MJ, Grytnes JA, Jurasinski G, *et al.*: **Accelerated increase in plant species richness on mountain summits is linked to warming.** *Nature.* 2018; **556**(7700): 231–234.
PubMed Abstract | Publisher Full Text

89. Feeley KJ, Silman MR, Bush MB, *et al.*: **Upslope migration of Andean trees.** *J Biogeogr.* 2011; **38**(4): 783–791.
Publisher Full Text

90. Burgess ND, Butynski TM, Cordeiro NJ, *et al.*: **The biological importance of the Eastern Arc Mountains of Tanzania and Kenya.** *Biol Conserv.* 2007; **134**(2): 209–231.
Publisher Full Text

91. Telwala Y, Brook BW, Manish K, *et al.*: **Climate-induced elevational range shifts and increase in plant species richness in a himalayan biodiversity epicentre.** *PLoS One.* 2013; **8**(2): e57103.
PubMed Abstract | Publisher Full Text | Free Full Text

92. Xu J, Badola R, Chettri N, *et al.*: **Sustaining biodiversity and ecosystem services in the Hindu Kush Himalaya.** In: *The Hindu Kush Himalaya Assessment Mountains, Climate Change, Sustainability and People.* (eds. Wester, P., Mishra, A., Mukherji, A. & Shrestha, A. B.), 2019.
Publisher Full Text

93. Gunawardene NR, Daniels AED, Gunatilleke IAUN, *et al.*: **A brief overview of the Western Ghats – Sri Lanka biodiversity hotspot.** *Curr Sci.* 2007; **93**(11).
Reference Source

94. Sorte FAL, Jetz W: **Projected range contractions of montane biodiversity under global warming.** *Proc Biol Sci.* 2010; **277**(1699): 3401–3410.
PubMed Abstract | Publisher Full Text | Free Full Text

95. Gonzalez P, Neilson RP, Lenihan JM, *et al.*: **Global patterns in the vulnerability of ecosystems to vegetation shifts due to climate change.** *Glob Ecol Biogeogr.* 2010; **19**(6): 755–768.
Publisher Full Text

96. IPCC: **Summary for Policymakers.** In: *Climate Change 2021: The Physical Science Basis. Contribution of Working Group I to the Sixth Assessment Report of the Intergovernmental Panel on Climate Change.* IPCC, 2021.
Publisher Full Text

97. Loarie SR, Duffy PB, Hamilton H, *et al.*: **The velocity of climate change.** *Nature.* 2009; **462**(7276): 1052–1055.
PubMed Abstract | Publisher Full Text

98. Malhi Y, Franklin J, Seddon N, *et al.*: **Climate change and ecosystems: threats, opportunities and solutions.** *Philos Trans R Soc Lond B Biol Sci.* 2020; **375**(1794): 20190104.
PubMed Abstract | Publisher Full Text | Free Full Text

99. Kjellstrom T, *et al.*: **Working on a warmer planet: the impact of heat stress on labour productivity and decent work**. International Labour Office, Geneva, 2019.
Reference Source

100. Gottfried M, Pauli H, Futschik A, *et al.*: **Continent-wide response of mountain vegetation to climate change.** *Nat Clim Chang.* 2012; **2**: 111–115.
Publisher Full Text

101. Berner LT, Massey R, Jantz P, *et al.*: **Summer warming explains widespread but not uniform greening in the arctic tundra bome.** *Nat Commun.* 2020; **11**(1): 4621.
PubMed Abstract | Publisher Full Text | Free Full Text

102. Metzger M, Bunce RGH, *et al.*: **A high resolution bioclimate map of the world.** *GLOBAL ECOL BIOGEOGR.* IN PRESS, 2012.

103. Zomer RJ, Trabucco A, Metzger M, *et al.*: **Environmental Stratification and projected climate change impacts on ecosystems in the Kailash Sacred Landscape of China, India, Nepal.** *ICIMOD.* 2012.

104. Gaire NP, Fan ZX, Chhetri PK, *et al.*: **Treeline dynamics in Nepal Himalaya in a response to complexity of factors.** *Ecology of Himalayan Treeline Ecotone.* 2023; 519–563.
Publisher Full Text

105. Lenoir J, Svenning JC: **Climate-related range shifts – a global multidimensional synthesis and new research directions.** *Ecography.* 2015; **38**: 15–28.
Publisher Full Text

106. Pecl GT, Araújo MB, Bell JD, *et al.*: **Biodiversity redistribution under climate change: impacts on ecosystems and human well-being.** *Science.* 2017; **355**(6332): eaai9214.
PubMed Abstract | Publisher Full Text

107. Elsen PR, Tingley MW: **Global mountain topography and the fate of montane species under climate change.** *Nat Clim Chang.* 2015; **5**: 772–776.
Publisher Full Text

108. Corlett RT, Westcott DA: **Will plant movements keep up with climate change?** *Trends Ecol Evol.* 2013; **28**(8): 482–488.
PubMed Abstract | Publisher Full Text

109. Ranjitkar S, Sujakhu NM, Lu Y, *et al.*: **Climate modelling for agroforestry species selection in Yunnan Province, China.** *Environ Model Softw.* 2016; **75**: 263–272.
Publisher Full Text

110. Parry ML, Rosenzweig C, Iglesias A, *et al.*: **Effects of climate change on global food production under SRES emissions and socio-economic scenarios.** *Glob Environ Change.* 2004; **14**(1): 53–67.
Publisher Full Text

111. DeFries R, Rosenzweig C: **Toward a whole-landscape approach for sustainable land use in the tropics.** *Proc Natl Acad Sci U S A.* 2010; **107**(46): 19627–19632.
PubMed Abstract | Publisher Full Text | Free Full Text

112. Zomer R, Trabucco A, Wang M, *et al.*: **Projected climate change impact on hydrology, bioclimatic conditions, and terrestrial ecosystems in the Asian Highlands**. 2016.
Publisher Full Text

113. Zomer RJ, Wang M, Xu J: **Projected climate change and impact on bioclimatic conditions in central and South-Central Asia - ICRAF East and Central Asia Research Report.** ICRAF Working Paper 187. World Agroforestry Centre East and Central Asia, Kunming, China. 2015; 1–50.
Publisher Full Text

114. Bezuijen M, Russel M, Zomer RJ, *et al.*: **Building the climate change resilience of Mongolia's blue pearl: the case study of Khuvsgul Lake National Park**. (Asian Development Bank, Manila, Phillipines), 2020.
Publisher Full Text

115. Mrema EM: **Towards the new post-2020 global biodiversity framework.** *Environmental Policy and Law.* 2021; **51**(1–2): 25–33.
Publisher Full Text

116. Zomer RJ, Trabucco A: **Future_Global_EnS: CMIP6 Global Environmental Stratification.** [Data set]. In Open Research Europe. *Zenodo.* 2025.
http://www.doi.org/10.5281/zenodo.15099763

Open Peer Review

Current Peer Review Status: ✔

Version 1

Reviewer Report 04 September 2025

https://doi.org/10.21956/openreseurope.22064.r57738

© **2025 Chetry V.** This is an open access peer review report distributed under the terms of the Creative Commons Attribution License, which permits unrestricted use, distribution, and reproduction in any medium, provided the original work is properly cited.

✔ **Vivek Chetry**
Gauhati University, Guwahati, Assam, India

This paper presents a global scale implementation of the Environmental Stratification (EnS) approach to forecast upcoming bioclimatic situations under climate change. Through the foundation of the well-established Global Environmental Stratification (GEnS) framework and combining results from 22 CMIP6 Earth System Models on four Shared Socioeconomic Pathways (SSPs), the authors generate the Future Global EnS database at 30 arc sec resolution.
The results demonstrate that by mid-century there is extensive reorganisation of bioclimates i.e. cooler boreal, temperate, and montane environments contract and shift poleward/upslope, while hotter and drier environments spread dramatically, especially with high-emissions scenarios.
The publicly available database stands as a useful asset for land-use planning, agricultural sustainability, biodiversity conservation, and climate adaptation. Significantly, the work offers both a methodological innovation (improved global stratification under climate change) and a working resource for research and decision-making.

Notable aspects
The study makes a timely and valuable contribution by updating the Global Environmental Stratification (GEnS) framework with CMIP6 climate projections and producing a high-res open-access database. Results are comprehensive and align well with observed ecological changes. The plain language summary is particularly effective and also the openly accessible dataset greatly enhances the utility of the work for biodiversity conservation, agriculture & land-use planning across global to local scales.

Areas for improvement
The paper would benefit from situating EnS more clearly alongside other classification frameworks like WWF ecoregions, to clarify its distinct advantages.
The utility for biodiversity conservation, land-use, and agriculture is well highlighted, but inclusion of one or two applied case examples would make the study more impactful.

overall, the article represents a rigorous and impactful piece of work.

Is the work clearly and accurately presented and does it cite the current literature?
Yes

Is the study design appropriate and does the work have academic merit?
Yes

Are sufficient details of methods and analysis provided to allow replication by others?
Yes

If applicable, is the statistical analysis and its interpretation appropriate?
Yes

Are all the source data underlying the results available to ensure full reproducibility?
Yes

Are the conclusions drawn adequately supported by the results?
Yes

Competing Interests: No competing interests were disclosed.

Reviewer Expertise: climate change, ecology, biodiversity conservation, landscape biology

I confirm that I have read this submission and believe that I have an appropriate level of expertise to confirm that it is of an acceptable scientific standard.